



**TITLE:** Predictions of Genotoxic Potential, Mode of Action, Molecular Targets, and Potency *via* a Tiered MultiFlow<sup>®</sup> Assay Data Analysis Strategy

**AUTHORS:** Stephen D. Dertinger<sup>1</sup>, Andrew R. Kraynak<sup>2</sup>, Ryan P. Wheeldon<sup>3</sup>, Derek T. Bernacki<sup>1</sup>, Steven M. Bryce<sup>1</sup>, Nikki Hall<sup>1</sup>, Jeffrey C. Bemis<sup>1</sup>, Sheila M. Galloway<sup>2</sup>, Patricia A. Escobar<sup>2</sup>, George E. Johnson<sup>3</sup>

**AFFILIATIONS:**

<sup>1</sup>Litron Laboratories, Rochester, NY, USA

<sup>2</sup>Merck & Co., Inc., West Point, PA, USA

<sup>3</sup>Institute of Life Science, Swansea University Medical School, Swansea University, SA2 8PP  
Wales, United Kingdom

**KEY WORDS:** TK6 cells, mode of action, multiplexed,  $\gamma$ H2AX, p53, clastogen, aneugen, benchmark dose

**RUNNING TITLE:** Tiered Data Analysis Strategy

This article has been accepted for publication and undergone full peer review but has not been through the copyediting, typesetting, pagination and proofreading process, which may lead to differences between this version and the Version of Record. Please cite this article as doi: 10.1002/em.22274

## ABSTRACT

The *in vitro* MultiFlow<sup>®</sup> DNA Damage Assay multiplexes  $\gamma$ H2AX, p53, phospho-histone H3, and polyploidization biomarkers into a single flow cytometric analysis [Bryce et al., 2016]. The current report describes a tiered, sequential data analysis strategy based on data generated from exposure of human TK6 cells to a previously described 85 chemical training set and a new pharmaceutical-centric test set (n=40). In each case, exposure was continuous over a range of closely spaced concentrations, and cell aliquots were removed for analysis following 4 and 24 hr of treatment. The first data analysis step focused on chemicals' genotoxic potential, and for this purpose we evaluated the performance of a machine learning (ML) ensemble, a rubric that considered fold increases in biomarkers against global evaluation factors (GEFs), and a hybrid strategy that considered ML and GEFs. This first tier further used ML output and/or GEFs to classify genotoxic activity as clastogenic and/or aneugenic. Test set results demonstrated the generalizability of the first tier, with particularly good performance from the ML ensemble: 35/40 (88%) concordance with *a priori* genotoxicity expectations and 21/24 (88%) agreement with expected mode of action (MoA). A second tier applied unsupervised hierarchical clustering to the biomarker response data, and these analyses were found to group certain chemicals, especially aneugens, according to their molecular targets. Finally, a third tier utilized benchmark dose analyses and MultiFlow biomarker responses to rank genotoxic potency. The relevance of these rankings is supported by the strong agreement found between benchmark dose values derived from MultiFlow biomarkers compared to those generated from parallel *in vitro* micronucleus analyses. Collectively, the results suggest that a tiered MultiFlow data analysis pipeline is capable of rapidly and effectively identifying genotoxic hazards while providing additional information that is useful for modern risk assessments—MoA, molecular targets, and potency.

## INTRODUCTION

Our laboratories have pursued the development and validation of a multiplexed flow cytometric assay that combines information from several biomarkers relevant to DNA damage response pathways and aneuploidy induction [Bryce et al., 2014, 2016, 2017, 2018; Bernacki et al., 2016]. This so-called MultiFlow<sup>®</sup> DNA Damage Assay is formatted as an add-and-read test that efficiently prepares cells in microtiter plates for flow cytometric analysis. The biomarkers measured are: i) phosphorylation of H2AX at serine 139 ( $\gamma$ H2AX) to detect DNA double strand breaks, ii) phosphorylation of histone H3 at serine 10 (p-H3) to identify mitotic cells, iii) nuclear p53 content as an indicator of p53 activation in response to DNA damage, iv) frequency of 8n+ cells to monitor polyploidization, and v) determination of nuclei counts to provide information about treatment-related cytotoxicity and cytostasis. Relative to individual, standard *in vitro* genotoxicity assays, an advantage of the MultiFlow method is that it goes beyond genotoxic hazard identification, since it is capable of distinguishing between clastogenic and aneugenic modes of action (MoA) [Bryce et al., 2016].

Given the multiplexed nature of the MultiFlow assay, the data analysis procedures used to synthesize and interpret biomarker responses have resembled pattern-recognition tools as opposed to parametric and non-parametric pair-wise tests that are commonly applied to traditional single endpoint genotoxicity assays. One published example of a MultiFlow data analysis strategy makes use of a series of global evaluation factors (GEFs) [Bryce et al., 2017]. This approach is based on cutoff response values that were derived for each biomarker and time point from data collected by 7 laboratories. To optimize agreement with *a priori* calls, a rubric was developed around the collection of cutoff values that categorizes chemicals as genotoxic or not, and if the former, whether the activity is clastogenic, aneugenic, or both. This approach was reported to exhibit good sensitivity and specificity across laboratories, and it provided reliable MoA information. However, an important caveat is that the initial report did not

evaluate the method's performance against chemicals that were outside of the training set, i.e., with an external test set that was not used to develop the GEFs and associated rubric.

Other data analysis strategies have made use of supervised machine learning (ML) tools. In this paradigm, mathematical algorithms were developed based on training set data where genotoxic potential and MoA are known. The labeled data provided a means to create models that could then be used to make predictions based on new biomarker response data that were not part of the training set. For instance, most recently, an ensemble of three ML algorithms consisting of logistic regression, random forest, and an artificial neural network has been described [Bryce et al., 2018]. In this case, a majority vote was used to make a final prediction about genotoxicity and genotoxic MoA. As with GEFs, this ML strategy also demonstrated good performance characteristics, but in this case in a more convincing fashion, as performance was maintained with an external test set of 103 chemicals.

Whereas there are certain advantages and disadvantages to the GEF and machine learning data analysis strategies, their use is not mutually exclusive, so it was of interest to evaluate them further, both in isolation and together. The current experiments were therefore designed to extend our work with MultiFlow data analysis strategies by testing the performance of the GEF rubric and/or a ML ensemble using chemicals outside the training set. Furthermore, we investigated the utility of hierarchical clustering to group genotoxic chemicals with similar molecular targets, and evaluated the capacity of MultiFlow biomarker responses to provide genotoxicity potency ranking. For these investigations, MultiFlow data were generated from TK6 cells exposed to a diverse set of chemicals using a continuous treatment design (i.e., 24 hr), and in some cases these analyses were supplemented with *in vitro* micronucleus measurements. The results are discussed in terms of the performance and benefits of a sequential, tiered, high information content data analysis pipeline (see Figure 1).

## MATERIALS AND METHODS

## Chemicals

The identities of 85 previously reported training set chemicals [Bryce et al., 2018] and a new set of pharmaceutical-centric test set chemicals (n=40), the source, and other information, are provided in Table I. Merck Sharp & Dohme Corp., a subsidiary of Merck & Co., Inc., Kenilworth, NJ, USA (MSD), supplied 20 of the 40 test chemicals (coded) to Litron, and these were stored at -20°C until they were solubilized in dimethyl sulfoxide (DMSO), at which point they were refrozen at -20°C. Additional test set chemicals (n = 20) were selected by Litron scientists largely from the list recommended by Kirkland and colleagues for evaluating new genotoxicity tests [Kirkland et al., 2016]. Our *a priori* expectation regarding the *in vitro* mammalian cell genotoxicity potential for each of the 125 chemicals can be found in Table I. As explained in more detail below, the experiments reported herein occurred in the absence of an exogenous metabolic activation system. Thus, the *a priori* calls provided in Table I reflect expected genotoxicity assay results in the context of an S9-free mammalian assay system.

## Cell Culture and Treatments

TK6 cells were purchased from ATCC® (cat. no. CRL-8015). Cells were grown in a humidified atmosphere at 37°C with 5% CO<sub>2</sub>, and were maintained at or below 1 x 10<sup>6</sup> cells/mL. The culture medium consisted of RPMI 1640 with 200 µg/mL sodium pyruvate (both from Sigma-Aldrich, St. Louis, MO), 200 µM L-glutamine, 50 units/mL penicillin and 50 µg/mL streptomycin (from Mediatech Inc., Manassas, VA), and 10% v/v heat-inactivated horse serum (Gibco®, a Thermo Fisher Scientific Company, Waltham, MA).

Chemicals selected by Litron scientists were tested using the same experimental design described previously [Bryce et al., 2016, 2017]. Briefly, treatments occurred in U-bottom 96 well plates, with 198 µL TK6 cell suspension (2 x 10<sup>5</sup>/mL) combined with 2 µL of DMSO-solubilized test chemical per well. The highest concentration tested was 1 mM, and the 19 additional concentrations were tested using a square root dilution scheme—that is, each concentration

differed from the one above by a factor of 70.71%. In this manner a wide range of concentrations were evaluated (i.e., nearly 3 orders of magnitude, 0.0014 to 1 mM). Each of the 20 concentrations was tested in a single well, whereas solvent was evaluated in 4 replicate wells. Upon addition of test chemical the plates were immediately incubated in a humidified atmosphere at 37°C with 5% CO<sub>2</sub> for 24 hr.

MSD-supplied chemicals were tested similarly, with the following exceptions. Preliminary dose-range finding experiments were used to generate 24 hr relative nuclei count (RNC) data for each chemical provided (*via* MultiFlow<sup>®</sup> — Cleaved PARP Kit, Litron Laboratories, Rochester, NY). Concentrations for the definitive experiment were chosen based on the RNC results with the intention to test at least one concentration that approached or slightly exceeded the MultiFlow assay's cytotoxicity limit, that is 80% reduction to RNC at 24 hr [Bryce et al., 2016]. There were two exceptions, 14n and 16p, compounds that were tested up to maximal feasible concentrations due to the low quantity of chemical that could be supplied (4.41 and 100 μM, respectively). For the definitive experiments, 10 concentrations of each chemical were tested in duplicate wells of a 96 well plate. As described above, the majority of chemicals were tested using a square root 2 dilution scheme. Based on data from preliminary dose-range finding experiments, some chemicals were tested using finer dilution schemes.

#### *MultiFlow Assay*

TK6 cells were prepared for analysis using reagents and instructions included in the MultiFlow<sup>®</sup> DNA Damage Kit — p53, γH2AX, Phospho-Histone H3 (Litron Laboratories, Rochester, NY). Components and preparation of the MultiFlow working solution have been described in detail previously [Bryce et al. 2016, 2017]. At the 4 and 24 hr sampling times, cells were resuspended with pipetting, then 25 μL were removed from each well and added to a new 96-well plate containing 50 μL/well of pre-aliquoted working MultiFlow reagent solution. Mixing

was accomplished by pipetting the contents of each well several times. After incubation at room temperature for 30 min, samples were analyzed *via* flow cytometry.

Flow cytometric analysis was carried out using either a FACSCanto™ II flow cytometer equipped with a BD™ High Throughput Sampler or a Miltenyi Biotec MACSQuant® Analyzer 10 flow cytometer with integrated 96-well MiniSampler device. Stock photomultiplier tube detectors and associated optical filter sets were used to detect fluorescence emissions associated with the fluorochromes: FITC (detected in the FITC channel, to use BD instrument parlance), PE (PE channel), propidium iodide (PerCP-Cy5.5 channel), and Alexa Fluor® 647 (APC channel).

Representative bivariate graphs, gating logic, and position of regions were described in detail in earlier reports [Bryce et al., 2016, 2017; Bernacki et al., 2016]. Briefly, two biomarker measurements,  $\gamma$ H2AX and p53, were based on the shift in median channel fluorescence intensity relative to same-plate solvent controls. Polyploidy and p-H3 biomarker measurements were based on their frequency among other nuclei. Nuclei to counting bead ratios were calculated for each sample, and these ratios were used to determine absolute nuclei counts (those with 2n and greater DNA-associated propidium iodide fluorescence). Nuclei counts were used to derive RNC, and %cytotoxicity was calculated as 100% minus %RNC at 24 hr.

#### *MultiFlow Data Analysis: Pre-Processing*

Data analyses described herein were restricted to those concentrations that did not exceed the MultiFlow assay's cytotoxicity limit, i.e., the top concentration of each chemical had to exhibit  $\leq 80\%$  reduction to RNC at the 24 hr time point. This has been described previously by Bryce and colleagues [2016, 2017]. The present report differs slightly, such that in addition to the 80% maximum cytotoxicity limit noted above, only two concentrations within the cytotoxicity range 70-80% were permitted. Finally, except for 14n and 16p as noted above, in the absence of excessive cytotoxicity the top concentration was 1 mM or the lowest precipitating concentration, whichever was lower.

For the GEF, machine learning, and benchmark dose analyses described below, 4 and 24 hr  $\gamma$ H2AX, p53, and p-H3 measurements, and 24 hr polyploidy frequencies, were converted to fold-change values by dividing them by the mean value associated with solvent-exposed cultures on the same plate (Microsoft Excel 2008, v12.3.6). This was performed for every test article concentration that was not excluded due to excessive cytotoxicity or other limits described above.

Unsupervised clustering analyses benefitted from several transformations. First, feature scaling (also known as unity-based normalization) was applied to every test article concentration to bring the values into the range 0 to 1 [Jayalakshmi and Santhakumaran, 2011]. Second, for each biomarker response and time point combination, fold-change values versus normalized concentration curves were used to generate an area under the curve (AUC) value. AUC provided a means of converting each biomarker dose-response relationship for every chemical into a single value. This was accomplished using Microsoft Excel *via* the trapezoidal rule as described at <https://calculushowto.com/find-the-area-under-the-curve-in-excel>. One (1) was subtracted from every biomarker's fold-change value before AUC calculations were made in order to set the no effect (baseline) value to zero. With this offset in place, AUC values were zero or nearly so in the case of no response, positive in the case of an increase, and negative in the case of a reduction. Also note that polyploid fold change values were transformed with the square root function, a processing step that converted this biomarker's dynamic range to one that more closely approximated that of the other biomarkers (found to be advantageous for artificial neural network models, see Bryce et al., 2018).

#### *MultiFlow Data Analysis: Global Evaluation Factors*

MultiFlow biomarker/time point combinations were compared to GEFs reported by Bryce and colleagues [2017]. GEFs for the three clastogen-responsive biomarkers 4 hr  $\gamma$ H2AX, 4 hr



p53, and 24 hr  $\gamma$ H2AX, were 1.51-, 1.40-, and 2.11-fold, respectively; GEFs for the three aneugen-responsive biomarkers 4 hr p-H3, 24 hr p-H3, and 24 hr polyploidy, were 1.71-, 1.52-, and 5.86-fold, respectively; and the GEF for the pan-genotoxicant (clastogen- and aneugen-responsive) biomarker, 24 hr p53, was 1.45-fold. Meeting or exceeding these interlaboratory-derived values identified a significant biomarker response at a particular time point. To synthesize the results of these multiple comparisons and to make judgments about genotoxic potential and MoA, the following rubric was applied. A genotoxic call with a clastogenic MoA required two successive concentrations to meet or exceed the GEF for at least two out of four clastogen-sensitive biomarkers: 4 hr  $\gamma$ H2AX, 4 hr p53, 24 hr  $\gamma$ H2AX, and 24 hr p53. A genotoxic call with an aneugenic MoA required two successive concentrations to meet or exceed the GEF for at least two out of four aneugen-sensitive biomarkers: 4 hr p-H3, 24 hr p-H3, 24 hr polyploidy, and 24 hr p53. In cases where both clastogen and aneugen call criteria were met, the call was genotoxic with a “mixed” MoA. When the above criteria were not met, the call was non-genotoxic under the test conditions.

#### *MultiFlow Data Analysis: Machine Learning Ensemble*

The development and use of three ML models, multinomial logistic regression (LR), artificial neural network (ANN), and random forest (RF), was described in detail previously [Bryce et al., 2018]. Briefly, these various models utilize 4 and 24 hr MultiFlow data fold-change values and predict whether a chemical exhibits genotoxic activity or not, and if present whether the genotoxicity occurs *via* a clastogenic, aneugenic, or clastogenic and aneugenic MoA. Each model's output was synthesized into genotoxicity and MoA calls as follows. Genotoxic, with evidence for a clastogenic MoA, required two successive concentrations to exhibit clastogen probability scores  $\geq 80\%$ , or one concentration to exhibit a clastogen probability score  $\geq 90\%$ . Genotoxic, with evidence for an aneugen MoA, required two successive concentrations to

exhibit aneugen probability scores  $\geq 80\%$ , or one concentration to exhibit an aneugen probability score  $\geq 90\%$ . Non-genotoxic was defined as the absence of two successive concentrations exhibiting clastogen or aneugen probability scores  $\geq 80\%$ , and no one concentration exhibiting a clastogen or aneugen probability score  $\geq 90\%$ .

A majority vote ensemble considered the genotoxicity calls from each of the 3 modeling approaches as described above. A simple majority (2 out of 3) was necessary for a summary genotoxic call. For most chemicals, MoA predictions were found to be in agreement across models. In instances when models showed significant clastogen and aneugen probabilities, the chemical was considered genotoxic with evidence for a mixed MoA.

#### *MultiFlow Performance Assessments*

Training and test set chemicals were evaluated against *a priori* genotoxicity and MoA expectations. This was accomplished by evaluating the performance of the GEF rubric and ML ensemble on their own. Furthermore, we investigated a hybrid strategy that made use of both GEFs and ML predictions. With this approach, an overall genotoxic call was made when *either* the GEF or ML ensemble was positive.

For each strategy described above, performance was assessed by determining the level of agreement between expected and observed genotoxicity calls. This was accomplished by calculating the percentage of chemicals correctly identified as being genotoxic or non-genotoxic. Furthermore, for those agents that were identified as genotoxic, the level of agreement between MoA calls was also made by calculating the percentage of compounds that showed expected MoA. In the several instances where *a priori* MoA was either difficult to define or hypothesized to be a mixed MoA, any genotoxic MoA prediction was considered correct. In cases where a presumably non-genotoxic chemical was identified as genotoxic, any/all associated MoA calls were considered incorrect.

### *Unsupervised Clustering*

Chemicals that were identified as aneugens by the hybrid GEF and machine learning approach were evaluated using JMP software's unsupervised clustering platform (JMP, v12.0.1). As described above, the biomarker response data were first converted to AUC values, and when clustering aneugens, the following 7 biomarkers were used as variables: 4 hr  $\gamma$ H2AX, p-H3 and p53, and 24 hr  $\gamma$ H2AX, p-H3, p53 and 24 hr polyploidy. The analysis options were set as follows: clustering method = hierarchical; method for calculating distances between clusters = "Ward"; data as usual = "Standardize Data"; data visualization = "Dendrogram", with "two way clustering".

Chemicals identified as clastogens by the hybrid GEF and machine learning approach were evaluated in a similar manner. However, in this case, the 4 variables were utilized: 4 hr  $\gamma$ H2AX, 4 hr p53, 24 hr  $\gamma$ H2AX, and 24 hr p53.

### *Benchmark Dose Analyses*

A subset of the reference genotoxic chemicals (n = 34) were evaluated for *in vitro* micronucleus (MN) formation using TK6 cells from the same treated cultures used in the MultiFlow assay. These analyses were conducted at the 24 hr time point, and were accomplished *via* flow cytometric analysis using *In Vitro* MicroFlow<sup>®</sup> Kit reagents (Litron Laboratories, Rochester, NY). These methods have been reported in detail elsewhere [Avlasevich *et al.*, 2006]. For the MN endpoint, concentrations were limited to those that resulted in  $\leq$  55% reduction to relative nuclei counts.

The Benchmark Dose (BMD) for continuous data is defined as the dose or exposure that results in a predetermined percent change (benchmark response, BMR) in the response rate of an adverse effect relative to the response in the concurrent controls, generally in the range of 1-10% increase in the background [MacGregor *et al.*, 2015]. Traditionally, the BMD approach is

utilized to estimate a Point of Departure (PoD) value from *in vivo* studies and thereby derive compound specific reference values in human health safety assessment; in these cases, the choice of BMR value should be justified. There is much debate over the appropriate BMR value to be selected, with several expert groups suggesting that an endpoint specific effect size approach is necessary [Slob, 2016; Zeller et al., 2016, 2017]. Briefly, a ‘one-size-fits-all’ BMR in the range of 1-10% is suggested to be inappropriate to apply to all endpoints. One theory favors scaling the BMR in percent change to the maximum response observed for the endpoint, which takes into account natural variation [Slob, 2016]. Based on a similar principle, work by Zeller et al. [2016] examined data from multiple genotoxicity endpoints to calculate endpoint specific ‘response quotients’ by dividing the assay’s response at a non-genotoxic dose level by the response of the concurrent vehicle control. The resulting fold-increase values over control were converted into BMR values in percent. Results of applying the approach to datasets derived from multiple *in vivo* genotoxicity studies range from 20-110%.

Importantly, it is not the purpose of this study to derive PoD metrics to infer reference values. Rather, we chose BMRs to minimize variation at the respective point in the dose response curve and thereby generate more precise PoD estimates [Slob and Setzer, 2014; Wills et al., 2015; Bemis et al., 2016]. Furthermore, the choice of BMR is not critical for *in vitro* endpoint comparisons, providing that it is the same value for all chemicals in the group. This has been demonstrated by Bemis and colleagues [2016], who produced BMD confidence intervals for various BMR values and showed similar correlations.

BMD analyses were performed for the subset of 34 chemicals with concurrent MultiFlow and MicroFlow data. Specifically,  $\gamma$ H2AX, p-H3, p53, and *in vitro* MN dose responses were evaluated using PROAST (v63.3). Values for Critical Effect Size (CES, in PROAST notation) of 0.5 (BMR 50%), or 1.0 (BMR 100%, in the case of *in vitro* MN compounds mitomycin C, 4-nitroquinoline 1-oxide, and topotecan—which failed to yield a dose response with BMR 50%) were used for BMD analysis for the compounds. Compound was selected as covariate per

endpoint and CES. The resulting 95% Confidence Intervals (CI's) were used to represent the relative potency of the compound for the endpoint under study. After ranking the *in vitro* MN induction potency of each compound, the data were compared with 24 hr  $\gamma$ H2AX and 24 hr p53 endpoints for the clastogen group of compounds, and 24 hr p-H3 and 24 hr p53 endpoints for the aneugen group of compounds. These correlations are represented in cross system plots on a double Log scale [Soeteman-Hernández et al, 2016; Bemis et al., 2016]. The analyses were conducted separately for clastogens (n = 21) and aneugens (n = 13).

Figure 1 is a schematic representation of the overall data analysis strategy that was configured into three tiers and applied to MultiFlow data as described in detail above.

## RESULTS AND DISCUSSION

### *Tier 1 Analyses: Training Set*

The 85 reference chemicals that comprise the training set were given *a priori* classifications in regard to their genotoxic potential, as well as their predominant genotoxic MoA, clastogenicity or aneugenicity (Table I). Results for several of these agents are presented in detail in order to describe prototypical response profiles, and to introduce a new data visualization tool. These examples should provide a useful background for interpreting the aggregate chemical results that are presented hereafter.

Thapsigargin is an inhibitor of the sarco/endoplasmic reticulum  $\text{Ca}^{++}$  ATPase [Rogers et al., 1995]. A radar plot portrays each biomarker response and time point combination as a function of concentration (Figure 2a). As expected for a non-genotoxicant, no substantial increases in  $\gamma$ H2AX, p-H3, p53 or polyploidization biomarkers were observed, despite that fact that it was tested to cytotoxic concentrations (71% cytotoxicity). Thus, it is not surprising that neither the GEF rubric or any of the three ML models predicted genotoxicity (Table II). Note that interested readers can access an Excel version of Table II as Supplemental file 1.

Treatment of TK6 cells with the reference genotoxicant 4-nitroquinoline 1-oxide resulted in a prototypical clastogenic response profile (Figure 2b). The  $\gamma$ H2AX biomarker was increased at 4 and 24 hr. Whereas p53 activation at the 24 hr time point is a pan-genotoxicity signal, activation at 4 hr, as observed here, is quite specific for clastogens [Bryce et al., 2014, 2016]. Additionally, 4-nitroquinoline 1-oxide did not increase polyploidization, and the p-H3 biomarker was reduced in a dose-dependent manner. Both of these observations provide additional evidence of clastogenic as opposed to aneugenic activity. As shown in Table II, the GEF rubric and all three of the ML models predicted genotoxicity, with a clastogenic MoA.

Mebendazole's aneugenicity has been attributed to microtubule binding [Laclette et al., 1980]. MultiFlow response data illustrate a typical tubulin binder-induced aneugenic response profile (Figure 2c). While anti- $\gamma$ H2AX-associated fluorescence did not increase at either time point and p53 translocation was not apparent at 4 hr, marked p53 responses were observed at 24 hr. Furthermore, robust increases in p-H3 positive events were induced by mebendazole, and this was accompanied by polyploidization. GEFs as well as the machine learning ensemble identified this compound as genotoxic, with evidence for an aneugenic MoA.

Crizotinib is another aneugen that is instructive for several reasons. Crizotinib is a potent inhibitor of c-Met and ALK (anaplastic lymphoma kinase), with cell-based assay IC50 values in the low nM range [Awad and Shaw, 2014]. Even so, there is evidence that the agent's *in vitro* aneugenic activity may be related to off-target effects on aurora kinase(s) [Kong et al., 2018]. Data presented in Figure 2d support this view, as it generated response profiles that are similar to several confirmed aurora kinase inhibitors tested in the MultiFlow assay (e.g., ZM-447439 and tozasertib). As with many tubulin binders, p53 activation and polyploidization were observed at the 24 hr time point. In the case of this kinase inhibitor, polyploidization was especially robust, and was evident well before the assay's cytotoxicity limit was reached (i.e., 8-fold increase in ploidy at 59% cytotoxicity). Unlike tubulin binders, the proportion of p-H3-positive events

was not elevated. Rather, at the highest concentrations tested, severe decreases were observed. These observations are consistent with aurora kinase inhibition, as this activity would be expected to repress serine 10 phosphorylation of histone H3 on mitotic chromosomes [Crosio et al., 2002]. Despite the response profile being quite different than spindle poisons, both the GEF rubric as well as all three of the ML models identified crizotinib as genotoxic, with evidence for an aneugenic MoA (Table II).

Results from the tier 1 data analyses are presented for all 85 training set chemicals in Table II. For the ML ensemble, the concordance between *a priori* expected and observed genotoxicity calls was 99%. For those agents with a genotoxic call, the agreement with expected MoA was 98%. In both cases, the one mischaracterized agent was imatinib mesylate (identified as a clastogen). Supplemental file 2a-c provides Manhattan-type plots that show ML probabilities for each of the 85 chemicals at every concentration tested.

Table II also provides performance metrics for GEFs. The most obvious difference between GEFs and ML is that the latter was effective for both genotoxicity calls and MoA predictions (at least with a training set size of 85 chemicals), while the GEF rubric showed a lower level of agreement between expected and observed genotoxic activity calls (i.e., 93% concordance), especially for clastogens. As shown by Table II, the hybrid strategy, GEF + ML, did not outperform ML on its own.

#### *Tier 1 Analyses: Test Set*

With promising results evident for 85 training set chemicals, work with compounds that were not used to devise the GEF rubric or the ML models were tested in the MultiFlow assay. The results from tier 1 analyses are presented in Table III. For this set of 40 diverse chemicals, the ML ensemble provided the best performance: 88% agreement between expected and observed genotoxicity calls. As with the training set, GEFs alone did not perform as well, as it resulted in 75% agreement with *a priori* classifications. Furthermore, the hybrid GEF + ML

strategy did not outperform the ML-only approach (88%).

Three suspected genotoxicants were not identified as such by any of the tier 1 analysis strategies that were evaluated: 6f, 13m, and 14n. While 6f was an anticipated aneugen, it was not observed to affect any of the aneugen-sensitive biomarkers, despite the fact that analyses included concentrations that induced up to 63.8% cytotoxicity. Compound 14n was also classified *a priori* as aneugenic, and in this case only one aneugen biomarker was slightly induced: 4 hr p-H3 was increased by 1.39-fold at the highest concentration tested, 4.41  $\mu\text{M}$ . This false negative result for 14n should be qualified to some degree, since cytotoxicity at the highest feasible concentration tested was 48.7%, well below the assay's cytotoxicity limit of 80%. The third false negative result, 13m, is also noteworthy. Whereas 6f and 14n showed slight to nil biomarker responses, 13m caused robust increases that exceeded biomarker GEFs for 4 hr p-H3 and 4 hr  $\gamma\text{H2AX}$  across several consecutive concentrations, as well as 24 hr polyploidy at the highest concentration (Figure 3a). This response profile was not observed in the 85 chemical training set, and consequentially the GEF rubric was not developed with this in mind, and the ML models have no experience with this pattern.

Tier 1 mischaracterized two non-genotoxicants as genotoxic: 2b and 12L. In the case of 2b (a.k.a., sodium diethyldithiocarbamate trihydrate), it should be noted that this compound has been shown to induce cytogenetic damage in both CHO and TK6 cells [Hilliard et al., 1998; Galloway et al., 1998; Greenwood et al., 2004], and DNA double strand breaks in rat hepatocytes [Storer et al., 1996], but genotoxicity was seen only at concentrations deemed overly cytotoxic by current testing standards. There are at least two biologically plausible causes for indirect effects leading to *in vitro* DNA damage: diethyldithiocarbamate chelates copper and zinc, and it is a potent inhibitor of superoxide dismutase [Heikkila et al., 1976; Nicotera et al., 1989].

Of the chemicals identified as genotoxic, tier 1 analyses were also used to predict their genotoxic MoA. As shown in Table III, ML resulted in 88% agreement between expected and



observed calls. GEF alone and the hybrid GEF + ML approaches performed similarly (88%). Note that interested readers can access an Excel version of Table III as Supplemental file 1. One compound, 16p, showed mixed activities, as both clastogen and aneugen biomarker responses were detected. This was an expected result, as 16p has an azobenzimidazole structure that was previously observed to induce premature centromere separation at metaphase in addition to induction of micronuclei and structural aberrations. MultiFlow biomarker results for this atypical agent are shown in Figure 3b. The three chemicals with misidentified MoA included the aneugen call for ciprofloxacin, a fluoroquinolone class antibiotic that was expected to exhibit clastogenic activity based on its reported topoisomerase II inhibitor activity, and the two *a priori* non-genotoxicants discussed above (i.e., 2b and 12L; both identified as clastogens).

Supplemental file 3a-c provides Manhattan-type plots that show machine learning probabilities for each of the 40 test set chemicals at every concentration evaluated. Overall, the high concordance values speak to the generalizability of the ML ensemble to detect genotoxicants, and to furthermore provide an indication of genotoxic MoA.

### Tier 2 Analyses

A set of 21 *a priori* aneugens and mixed MoA chemicals that were identified as such in tier 1 ML analyses were evaluated *via* unsupervised hierarchical clustering using 4 and 24 hr MultiFlow biomarker data that were each converted to a single AUC value. The resulting groupings are presented in Figure 4 in the form of a two dimensional dendrogram. The clade denoted “TB” was entirely comprised of tubulin binders. Note that whereas the exact mechanism of test agent 17q is not known, it is a benzimidazole-containing structure and therefore expected to have tubulin-binding properties. The other clear grouping is denoted “KI”, a clade that included each of the presumptive mitotic kinase inhibitors that were tested: AMG 900, crizotinib, tozasertib, hesperadin, ZM-447439, and 10j.

The set of 46 *a priori* clastogens that were identified as such in tier 1 analyses were also evaluated *via* unsupervised clustering using the 4 clastogen-responsive biomarkers. The results are shown in Figure 5. For this set of diverse clastogens, it is less obvious that clusters formed around different molecular targets. That said, the clade identified as “T1” was highly enriched for topoisomerase inhibitors (6/8), and the “C-L” grouping was enriched for DNA cross-linking agents (5/9).

Taken together, a second tier that consists of unsupervised hierarchical clustering appears to complement genotoxic potential and MoA analyses, as it provides useful information about likely molecular targets. This is especially true in the case of delineating aneugens that target mitotic kinases versus those that interfere with tubulin polymerization.

### *Tier 3 Analyses*

BMD metrics served as a basis for tier 3 analyses that were conducted to determine whether MultiFlow biomarker(s) could provide a reliable indication of chemicals’ genotoxic potency as measured by the *in vitro* micronucleus assay. The advantage of using BMD-derived potency metrics has been previously discussed by Soeteman-Hernández and colleagues [2015, 2016], and here we have expanded the utility to *in vitro* datasets. As shown in Figures 6, 7, and 8, the BMDs in the MultiFlow endpoints were plotted against micronucleus response BMDs on a double-log scale. As opposed to representing correlation with a numerical coefficient value, a linear relationship with intercept zero equals a straight line in a double-log plot. Therefore, two lines with unity slope were drawn on each correlation plot in such a manner that the majority of the BMD confidence intervals are encompassed between the lines. The distribution of BMD positions within the two lines show approximate linearity, differing by a proportionality constant. Furthermore, the vertical distance between the two lines translates into an uncertainty margin given by the estimation of a BMD on the y axis based on a specified BMD on the x axis, and vice versa. The uncertainty margin is used as a measure of correlation between two endpoints.

For the aneugens, when comparing MN induction to p53 responses, the cross system plots show good correlation, with the majority of the compounds located between the two lines (Figure 6). Taking the microtubule binder nocodazole as an example, the horizontal dashed line intersections with the sloped dashed lines may be considered as the respective upper and lower bounds of the uncertainty range for the *in vitro* MN endpoint. The intercepts of approximately -3 and -1 on the Log scale correspond to lower and upper bounds of  $10^{-3} = 0.001$  and  $10^{-1} = 0.1$   $\mu\text{M}$ , respectively. Hence, the *in vitro* MN BMD for nocodazole is estimated to lie between 0.001 and 0.1  $\mu\text{M}$  considering an uncertainty margin of approximately 1 Log. In fact, the *in vitro* MN potency for nocodazole in the dataset represented in Figure 6 has both BMDL and BMDU either side of -2 Log, and hence within the estimated potency of -3 Log and -1 Log estimated from the p53 response. The MN vs. 24 hr p-H3 system plot also indicates the BMDs for the majority of compounds in both systems are proportionally related (Figure 6), however the two lines are drawn further apart than the MN vs. 24 hr p53 system (i.e., 2 logs versus 1 log). In both cases, MN vs. p53 and MN vs. p-H3, the data are randomly scattered with good correlation.

For the clastogens, good correlation is observed for MN vs.  $\gamma\text{H2AX}$  and MN vs. p53, with data randomly scattered between the two diagonal lines of the unity slopes, with distances of approximately 3 Log, and 2 Log respectively for each system (Figure 7). The *in vitro* MN BMD100 CI for compounds mmc, nqo, and top, plotted against BMD50  $\gamma\text{H2AX}$  and p53 endpoints show similar correlation with BMD CIs lying within approximately 2 Log for both systems (Figure 8).

The correlations observed here are consistent with those of other genotoxicity endpoints which have been compared using similar methodologies. Bemis and colleagues [2016] obtained an uncertainty margin of approximately 1.5 Log when comparing the *in vitro* MN responses against *in vivo* MN responses for a group of 7 clastogens. Similarly, Soeteman-Hernández et al. [2015] assessed the ability to predict *in vivo* MN potency from *in vitro* MN data. BMD confidence

intervals spanned 2 orders of magnitude, with *in vivo* BMD confidence intervals generally showing smaller than those from *in vitro* studies.

### Conclusions

The MultiFlow DNA Damage Assay's ability to predict chemicals' *in vitro* genotoxic potential and MoA was demonstrated with an external test set of 40 largely pharmaceutical-centric compounds. Whereas the GEF and associated rubric exhibited high specificity and accurate MoA predictions, it provided lower sensitivity to detect genotoxicants relative to a ML ensemble. Indeed, ML exhibited a good balance between genotoxic potential predictions and MoA information. Interestingly, a hybrid strategy whereby GEFs and ML were used to make calls was no better than ML on its own. That being said, from a practical perspective, GEFs may serve a useful function at novice laboratories. GEFs can be used right away, even as training set data are being generated. Furthermore, while early ML models are being built and tested, concurrent use of the GEF rubric represents a safety net of sorts, as it is capable of highlighting biomarker response patterns that the machine learning model(s) may not have encountered. On a related point, additional practical advice for new adopters of this assay is provided in Supplemental file 4, that is, a shorter list of diverse training set chemicals (n = 24) that can be used to build base learner(s).

Unsupervised clustering is able to group certain genotoxicants with the same or similar molecular targets based on multifactorial biomarker response patterns. This was especially successful with aneugens that were clustered into tubulin binder and kinase inhibitor groups. While these analyses do not offer proof of molecular targets, they do represent a powerful hypothesis-generating tool, one that could be used to efficiently design the necessary follow-up test(s) aimed at directly and conclusively identifying molecular target(s) responsible for *in vitro* genotoxicity

With respect to the BMD analyses reported herein, the strong correlation of MultiFlow

biomarkers to *bona fide* genomic damage in the form of MN provides assurances of the relevance of the new assay's endpoints. Furthermore, the correlations suggest that potency determinations based on MultiFlow endpoints, at least on a rank-order basis, are likely comparable to those derived from the MN assay. This bolsters the use case whereby the constellation of MultiFlow assay biomarkers serve as a reliable genotoxicity screening tool that is predictive of *in vitro* MN formation, with the benefit of providing more mechanistic information. Finally, dose-response analyses such as these are worth pursuing further because they reflect the paradigm shift that has been transitioning genotoxicity away from a simple binary yes/no characteristic to a quantitative metric that has the potential to better inform risk assessments as margin of exposure and other toxicological principles can be considered [Pottenger and Gollapudi, 2009, 2010; Gollapudi et al., 2013; Johnson et al., 2014; MacGregor et al., 2015a,b; Dearfield et al., 2017].

#### **AUTHOR CONTRIBUTIONS**

All authors contributed to experimental design. ARK, SMG and PAE selected 20 chemicals for testing, provided the coded chemicals, and subsequent to testing shared information about the chemicals' behavior in standard genetic toxicology assays. JCB oversaw receipt, storage and proper disposal of test chemicals. DTB and SMB performed benchtop work. DTB, SMB, NH, JCB and SDD each contributed to the statistical analyses strategy described herein. RPW and GEJ performed benchmark dose analyses and compared MultiFlow assay biomarker responses against micronucleus induction. SDD provided a first draft of the manuscript, and all authors contributed to the substantial revisions that followed.

#### **CONFLICT OF INTEREST STATEMENT**

DTB, SMB, NH, JCB, and SDD are employed by Litron Laboratories. Litron has a patent covering the flow cytometry-based assay described in this manuscript and sells a commercial kit

based on these procedures: MultiFlow<sup>®</sup> DNA Damage Kit—p53,  $\gamma$ H2AX, Phospho-Histone H3.

## ACKNOWLEDGMENTS

This work was funded in part by a grant from the National Institute of Health/National Institute of Environmental Health Sciences (NIEHS; grant no. R44ES029014). The contents are solely the responsibility of the authors, and do not necessarily represent the official views of the NIEHS.

## REFERENCES

- Attia SM, Aleisa AM, Bakheet SA, Al-Yahya AA, Al-Rejaie SS, Ashour AE, Al-Shabanah OA. 2009. Molecular cytogenetic evaluation of the mechanism of micronucleus formation induced by camptothecin, topotecan, and irinotecan. *Environ Mol Mutagen* 50:145-151.
- Avlasevich SL, Bryce SM, Cairns SE, Dertinger SD. 2006. In vitro micronucleus scoring by flow cytometry: differential staining of micronuclei versus apoptotic and necrotic chromatin enhances assay reliability. *Environ Mol Mutagen* 47:56-66.
- Awad MM, Shaw AT. 2014. ALK inhibitors in non-small cell lung cancer: Crizotinib and beyond. *Clin Adv Hematol Oncol* 12:429-439.
- Aydemir N, Bilaloğlu R. 2003. Genotoxicity of two anticancer drugs, gemcitabine and topotecan, in mouse bone marrow in vivo. *Mutat Res* 537:43-51.
- Bemis JC, Willis JW, Bryce SM, Torous DK, Dertinger SD, Slob W. 2016. Comparison of in vitro and in vivo clastogenic potency based on benchmark dose analysis of flow cytometric micronucleus data. *Mutagenesis* 31:277–285.
- Bernacki DT, Bryce SM, Bemis JC, Kirkland D, Dertinger SD. 2016.  $\gamma$ H2AX and p53 responses in TK6 cells discriminate promutagens and nongenotoxicant in the presence of rat liver S9. *Environ Mol Mutagen* 57:546-558.

- Bryce SM, Bemis JC, Mereness JA, Spellman RA, Moss J, Dickinson D, Schuler MJ, Dertinger SD. 2014. Interpreting in vitro micronucleus positive results: simple biomarker matrix discriminates clastogens, aneugens, and misleading positive agents. *Environ Mol Mutagen* 55:542–555.
- Bryce SM, Bernacki DT, Bemis JC, Dertinger SD. 2016. Genotoxic mode of action predictions from a multiplexed flow cytometric assay and a machine learning approach. *Environ Mol Mutagen* 57:171-189.
- Bryce SM, Bernacki DT, Bemis JC et al. 2017. Interlaboratory evaluation of a multiplexed high information content in vitro genotoxicity assay. *Environ Mol Mutagen* 58:146-161.
- Bryce SM, Bernacki DT, Smith-Roe SL, Witt KL, Bemis JC, Dertinger SD. 2018. Investigating the generalizability of the MultiFlow® DNA damage assay and several machine learning models with a set of 103 diverse test chemicals. *Toxicol Sci* 162:146-166.
- Cheung JR, Dickinson DA, Moss J, Schuler MJ, Spellman RA, Heard PL. Histone markers identify the mode of action for compounds positive in the TK6 micronucleus assay. *Mutat Res* 777:7-16.
- Chinnasamy N, Rafferty JA, Hickson I, Ashby J, Tinwell H, Margison GP, Dexter TM, Fairbairn LJ. 1997. O6-benzylguanine potentiates the in vivo toxicity and clastogenicity of temozolomide and BCNU in mouse bone marrow. *Blood* 89:1566-73.
- Cimino MC. 2006. Comparative overview of current international strategies and guidelines for genetic toxicology testing for regulatory purposes. *Environ Mol Mutagen* 47:362–390.
- Cojocel C, Novotny L, Vachalkova A. 2006. Mutagenic and carcinogenic potential of menadione. *Neoplasma* 53:316-323.
- Crosio C, Fimia GM, Loury R, Kimura M, Okano Y, Zhou H, Sen S, Allis CD, Sassone-Corsi P. 2002. Mitotic phosphorylation of histone H3: spatio-temporal regulation by mammalian Aurora kinases. *Mol Cell Biol* 22:874-885.

- Curry PT, Kropko ML, Garvin JR, Fiedler RD, Theiss JC. 1996. In vitro induction of micronuclei and chromosome aberrations by quinolones: possible mechanisms. *Mutat Res* 352:143-150.
- Dearfield KL, Gollapudi BB, Bemis JC et al. 2017. Next generation testing strategy for assessment of genomic damage: A conceptual framework and considerations. *Environ Mol Mutagen* 58:264-283.
- de Graaf AO, van den Heuvel LP, Dijkman HB, de Abreu RA, Birkenkamp KU, de White T, van der Reijden BA, Smeitink JA, Jansen JH. 2004. Bcl-2 prevents loss of mitochondria in CCCP-induced apoptosis. *Exp Cell Res* 299:533-540.
- Degrassi F, De Salvia R, Berghella L. 1993. The production of chromosomal alterations by  $\beta$ -lapachone, an activator of topoisomerase I. *Mutat Res* 288:263-267.
- DeMarini DM, Brock KH, Doerr CL, Moore MM. 1987. Mutagenicity and clastogenicity of teniposide (VM-26) in L5178Y/TK +/- 3.7.2C mouse lymphoma cells. *Mutat Res* 187:141-149.
- Dertinger SD, Phonethepswath S, Weller P, Avlasevich S, Torous DK, Mereness JA, Bryce SM, Bemis JC, Bell S, Portugal S, et al. 2011. Interlaboratory *Pig-a* gene mutation assay trial: Studies of 1,3-propane sultone with immunomagnetic enrichment of mutant erythrocytes. *Environ Mol Mutagen* 52:748–755.
- Dertinger SD, Phonethepswath S, Avlasevich SL, Torous DK, Mereness J, Bryce SM, Bemis JC, Bell S, Weller P, MacGregor JT. 2012. Efficient monitoring of in vivo *Pig-a* gene mutation and chromosomal damage: Summary of 7 published studies and results from 11 new reference compounds. *Toxicol Sci* 130:328-348.
- Diaz D, Scott A, Carmichael P, Shi W, Costales C. 2007. Evaluation of an automated in vitro micronucleus assay in CHO-K1 cells. *Mutat Res*. 630:1-13.



Floxin [package insert]. Raritan, NJ: Ortho-McNeil, 2008.

[http://www.accessdata.fda.gov/drugsatfda\\_docs/label/2008/019735s059lbl.pdf](http://www.accessdata.fda.gov/drugsatfda_docs/label/2008/019735s059lbl.pdf).

Accessed October 12, 2018.

Futami T, Miyagishi M, Taira K. 2005. Identification of a network involved in thapsigargin-induced apoptosis using a library of small interfering RNA expression vectors. *J Biol Chem* 280:826-831.

Galloway SM, Aardema MJ, Ishidate Jr M, Ivett JL, Kirkland DJ, Morita T, Mosesso P, Sofuni T. 1994. Report from working group on *in vitro* tests for chromosomal aberrations. *Mutat Res* 312:241-261.

Galloway SM, Miller JE, Armstrong MJ, Bean CL, Skopek TR, Nichols WW. 1998. DNA synthesis inhibition as an indirect mechanism of chromosome aberrations: Comparison of DNA-reactive and non-DNA-reactive clastogens. *Mutat Res* 400:169-186.

Garcia-Canton C, Anadon A, Meredith C. 2013. Assessment of the *in vitro*  $\gamma$ H2AX assay by high content screening as a novel genotoxicity test. *Mutat Res* 757:158-166.

Gewirtz DA. 1999. A critical evaluation of the mechanisms of action proposed for the antitumor effects of the anthracycline antibiotics adriamycin and daunorubicin. *Biochem Pharmacol* 57:727-741.

Gleevec [package insert]. East Hanover, NJ: Novartis, 2001.

[http://www.accessdata.fda.gov/drugsatfda\\_docs/label/2008/021588s024lbl.pdf](http://www.accessdata.fda.gov/drugsatfda_docs/label/2008/021588s024lbl.pdf).

Accessed October 12, 2018.

Glover TW, Berger C, Coyle J, Echo B. 1984. DNA polymerase alpha inhibition by aphidicolin induces gaps and breaks at common fragile sites in human chromosomes. *Hum Genet* 67:136-142.

Gocke E, Bürgin H, Müller L, Pfister T. 2009. Literature review on the genotoxicity, reproductive toxicity, and carcinogenicity of ethyl methanesulfonate. *Toxicol Lett* 190:254-265.

- Gollapudi BB, Johnson GE, Hernández LG et al. 2013. Quantitative approaches for assessing dose-response relationships in genetic toxicology studies. *Environ Mol Mutagen* 54:8-18.
- Gollapudi P, Hasegawa LS, Eastmond DA. 2014. A comparative study of the aneugenic and polyploidy-inducing effects of fisetin and two model Aurora kinase inhibitors. *Mutat Res* 767:37-43.
- Greenwood SK, Hill RB, Sun JT, Armstrong MJ, Johnson TE, Gara JP, Galloway SM. 2004. Population doubling: A simple and more accurate estimation of cell growth suppression in the in vitro assay for chromosomal aberrations that reduces irrelevant positive results. *Environ Mol Mutagen* 43:36-44.
- Gulati DK, Witt K, Anderson B, Zeiger E, Shelby MD. 1989. Chromosome aberration and sister chromatid exchange tests in Chinese Hamster Ovary cells in vitro III: Results with 27 chemicals. *Environ Mol Mutagen* 13:133-193.
- Han C, Nam MK, Park HJ, Seong YM, Kang S, Rhim H. 2008. Tunicamycin-induced ER stress upregulates the expression of mitochondrial HtrA2 and promotes apoptosis through the cytosolic release of HtrA2. *J Microbiol Biotechnol* 18:1197-1202.
- Henderson L, Fedyk J, Windebank S, Smith M. 1993. Induction of micronuclei in rat bone marrow and peripheral blood following acute and subchronic administration of azathioprine. *Mutat Res* 291:79-85.
- Hilliard C, Armstrong M, Bradt C, Hill R, Greenwood S, Galloway S. 1998. Chromosome aberrations in vitro related to cytotoxicity of non-mutagenic chemicals. *Environ Mol Mutagen* 31:316-326.
- IARC monograph, Clofibrate: <http://monographs.iarc.fr/ENG/Monographs/vol66/mono66-17.pdf>. Accessed October 12, 2018.
- Jayalakshmi T, Santhakumaran A. 2011. Statistical normalization and back propagation for classification. *International Journal of Computer Theory and Engineering* 3:89-93.

- Johnson GE, Soeteman-Hernández LG, Gollapudi BB et al. 2014. Derivation of point of departure (PoD) estimates in genetic toxicology studies and their potential applications in risk assessment. *Environ Mol Mutagen* 55:609-23.
- Hauf S, Cole RW, LaTerra S, Zimmer C, Schnapp G, Walter R, Heckel A, van Meel J, Rieder CL, Peters JM. 2003. The small molecule Hesperadin reveals a role for Aurora B in correcting kinetochore-microtubule attachment and in maintaining the spindle assembly checkpoint. *J Cell Biol* 161:281-294.
- Heard PL, Rubitski EE, Spellman RA, Schuler MJ. 2013. Phenolphthalein induces centrosome amplification and tubulin depolymerization in vitro. *Environ Mol Mutagen* 54:308-316.
- Heikkila RE, Cabbat FS, Cohen G. 1976. In vivo inhibition of Superoxide dismutase in mice by diethyldithiocarbamate. *J Biol Chem* 251:2182-2185.
- Hernández LG, van Benthem J, Johnson GE. 2013. A mode-of action approach for the identification of genotoxic carcinogens. *PLOS ONE* 8:e64532.  
doi:10.1371/journal.pone.0064532.
- Keshava C, Keshava N, Whong WZ, Nath J, Ong TM. 1998. Inhibition of methotrexate-induced chromosomal damage by folic acid in V79 cells. *Mutat Res* 397:221-228.
- Kimura A, Miyata A, Honma M. 2013. A combination of in vitro comet assay and micronucleus test using human lymphoblastoid TK6 cells. *Mutagenesis* 28:583-90.
- Kirkland D, Kasper P, Müller L, Corvi R, Speit G. 2008. Recommended lists of genotoxic and non-genotoxic chemicals for assessment of the performance of new or improved genotoxicity tests: a follow-up to an ECVAM workshop. *Mutat Res* 653:99-108.
- Kirkland D, Kasper P, Martus H-J, Müller L, van Benthem J, Madia F, Corvi R. 2016. Updated recommended lists of genotoxic and non-genotoxic chemicals for assessment of the performance of new or improved genotoxicity tests. *Mutat Res* 795:7-30.
- Klein CB, King AA. 2007. Genistein genotoxicity: Critical considerations of in vitro exposure dose. *Toxicol Appl Pharmacol* 224:1-11.

- Krishna G, Urda G, Tefera W, Lalwani ND, Theiss J. 1995. Simultaneous evaluation of dexamethasone-induced apoptosis and micronuclei in rat primary spleen cell cultures. *Mutat Res.* 332:1-8.
- Kondo Y, Honda S, Nakajima M, Miyahana K, Hayashi M, Shinagawa Y, Sato S, Inoue K, Nito S, Ariyuki F. 1992. Micronucleus test with vincristine sulfate and colchicine in peripheral blood reticulocytes of mice using acridine orange supravital staining. *Mutat Res* 278:187-191.
- Kong Y, Bender A, Yan A. 2018. Identification of novel aurora kinase A (AURKA) inhibitors via hierarchical ligand-based virtual screening. *J Chem Inf Model* 58:36-47.
- Kurihara D, Matsunaga S, Kawabe A, Fujimoto S, Noda M, Uchiyama S, Fukui K. 2006. Aurora kinase is required for chromosome segregation in tobacco BY-2 cells. *Plant J* 48:572-580.
- Laclette JP, Guerra G, Zetina C. 1980. Inhibition of tubulin polymerization by mebendazole. *Biochem Biophys Res Commun* 92:417-423.
- Li Y, Luan Y, Qi X, Li M, Gong L, Xue X, Wu X, Wu Y, Chen M, Xing G, Yao J, Ren J. 2010. Emodin triggers DNA double-strand breaks by stabilizing topoisomerase II-DNA cleavage complexes and by inhibiting ATP hydrolysis of topoisomerase II. *Toxicol Sci* 118:435-443.
- Lidoderm [package insert]. Chad's Ford, PA: Endo Pharmaceuticals, 2004.  
[http://www.accessdata.fda.gov/drugsatfda\\_docs/label/2005/020612s007lbl.pdf](http://www.accessdata.fda.gov/drugsatfda_docs/label/2005/020612s007lbl.pdf).  
Accessed October 12, 2018.
- Lotz AS, Havla JB, Richter E, Frölich K, Staudenmaier R, Hagen R, Kleinsasser NH. 2009. Cytotoxic and genotoxic effects of matrices for cartilage tissue engineering. *Toxicol Lett* 190:128-33.
- Lu P-Z, Lai C-Y, Chan W-H. 2008. Caffeine induces cell death via activation of apoptotic signal and inactivation of survival signal in human osteoblasts. *Int J Mol Sci* 9:698-718.

Lynparza [package insert]. Wilmington, DE: AstraZeneca Pharmaceuticals LP, 2014.

[http://www.accessdata.fda.gov/drugsatfda\\_docs/label/2014/206162lbl.pdf](http://www.accessdata.fda.gov/drugsatfda_docs/label/2014/206162lbl.pdf). Accessed October 12, 2018.

MacGregor JT, Frötschl R, White PA et al. 2015a. IWGT report on quantitative approaches to genotoxicity risk assessment I. Methods and metrics for defining exposure-response relationships and points of departure (PoDs). *Mutat Res* 783:55-65.

MacGregor JT, Frötschl R, White PA et al. 2015b. IWGT report on quantitative approaches to genotoxicity risk assessment II. Use of point-of-departure (PoD) metrics in defining acceptable exposure limits and assessing human risk. *Mutat Res* 783:66-78.

Martelli A, Allavena A, Campart GB, Canonero R, Ghia M, Mattioli F, Mereto E, Robbiano L, Brambilla G. 1995. In vitro and in vivo testing of hydralazine genotoxicity. *J Pharmacol Exp Ther* 273:113-120.

Matsushima T, Hayashi M, Matsuoka A, Ishidate M Jr, Miura KF, Shimizu H, Suzuki Y, Morimoto K, Ogura H, Mure K, Koshi K, Sofuni T. 1999. Validation study of the in vitro micronucleus test in a Chinese hamster lung cell line (CHL/IU). *Mutagenesis* 14:569-80.

Mevacor [package insert]. Whitehouse Station, NJ, USA: Merck Sharp & Dohme Corp., 2012. [http://www.accessdata.fda.gov/drugsatfda\\_docs/label/2012/019643s085lbl.pdf](http://www.accessdata.fda.gov/drugsatfda_docs/label/2012/019643s085lbl.pdf). Accessed October 12, 2018.

Moon JL, Kim SY, Shin SW, Park J-W. 2012. Regulation of brefeldin A-induced ER stress and apoptosis by mitochondrial NADP<sup>+</sup>-dependent isocitrate dehydrogenase. *Biochem Biophys Res Commun* 417:760-764.

Muehlbauer PA, Spellman RA, Gunther WC, Sanok KE, Wiersch CJ, O'Lone SD, Dobo KL, Schuler MJ. 2008. Improving dose selection and identification of aneugens in the in vitro chromosome aberration test by integration of flow cytometry-based methods. *Environ Mol Mutagen* 49:318-327.

National Toxicology Program Report, 6-Thioguanine:

<https://ntp.niehs.nih.gov/testing/status/agents/ts-m890081.html>. Accessed October 12, 2018.

National Toxicology Program Report, Sodium Dodecyl Sulfate:

<http://ntp.niehs.nih.gov/testing/status/agents/ts-10604-g.html>. Accessed October 12, 2018.

Nicotera TM, Notaro J, Notaro S, Schumer J, Sandberg AA. 1989. Elevated superoxide dismutase in Bloom Syndrome: A genetic condition of oxidative stress. *Cancer Res* 49:5239-5243.

Nikolova T, Dvorak M, Jung F, Adam I, Krämer E, Gerhold-Ay A, Kaina B. 2014.  $\gamma$ H2AX assay for genotoxic and nongenotoxic agents: Comparison of H2AX phosphorylation with cell death response. *Toxicol Sci* 140:103-117.

Oliver J, Meunier JR, Awogi T, Elhajouji A, Ouldelhkim MC, Bichet N, Thybaud V, Lorenzon G, Marzin D, Lorge E. 2006. SFTG international collaborative study on in vitro micronucleus test V. Using L5178Y cells. *Mutat Res* 607:125-152.

Parry EM, Parry JM, Corso C, Doherty A, Haddad F, Hermine TF, Johnson G, Kayani M, Quick E, Warr T, Williamson J. 2002. Detection and characterization of mechanism of action of aneugenic chemicals. *Mutagenesis* 17:509-521.

Paulsson B, Kotova N, Grawé J, Henderson A, Granath F, Golding B, Törnqvist M. 2003. Induction of micronuclei in mouse and rat by glycidamide, genotoxic metabolite of acrylamide. *Mutat Res* 535:15-24.

Paxil [package insert]. Research Triangle Park, NC: GlaxoSmithKline, 2011.

[http://www.accessdata.fda.gov/drugsatfda\\_docs/label/2011/020031s058s066.020710s022s030lbl.pdf](http://www.accessdata.fda.gov/drugsatfda_docs/label/2011/020031s058s066.020710s022s030lbl.pdf). Accessed October 12, 2018.

Payton M, Bush TL, Chung G, Ziegler B, Eden P, McElroy P, Ross S, Cee VJ, Deak HL, Hodous BL, Nguyen HN et al. 2010. Preclinical evaluation of AMG 900, a novel potent and highly selective pan-aurora kinase inhibitor with activity in taxane-resistant tumor

cell lines. *Cancer Res* 70:9846-9854.

Pepcid [package insert]. Whitehouse Station, NJ, USA: Merck Sharp & Dohme Corp., 2011.

[http://www.accessdata.fda.gov/drugsatfda\\_docs/label/2011/019462s037lbl.pdf](http://www.accessdata.fda.gov/drugsatfda_docs/label/2011/019462s037lbl.pdf).

Accessed October 12, 2018.

Pottenger LH and Gollapudi BB. 2009. A case for a new paradigm in genetic toxicology testing.

*Mutat Res* 678:148-151.

Pottenger LH and Gollapudi BB. 2010. Genotoxicity testing: Moving beyond qualitative “screen

and bin” approach towards characterization of dose-response and thresholds. *Environ Molec Mutagen* 51:792-799.

Rogers TB, Inesi G, Wade R, Lederer WJ. 1995. Use of thapsigargin to study Ca<sup>2+</sup>

homeostasis in cardiac cells. *Biosci Rep* 15:341-349.

Rosefort C, Fauth E, Zanki H. 2004. Micronuclei induced by aneugens and clastogens in

mononucleate and binucleate cells using the cytokinesis block assay. *Mutagenesis* 19:277-284.

Schuler M, Muehlbauer P, Guzzie P, Eastmond DA. 1999. Noscapine hydrochloride disrupts the

mitotic spindle in mammalian cells and induces aneuploidy as well as polyploidy in cultured human lymphocytes. *Mutagenesis* 14:51-56.

Smart DJ, Halicka HD, Schmuck G, Traganos F, Darzynkiewicz Z, Williams GM. 2008.

Assessment of DNA double-strand breaks and gammaH2AX induced by the topoisomerase II poisons etoposide and mitoxantrone. *Mutat Res* 641:43-47.

Slob W. 2016. A general theory of effect size, and its consequences for defining the benchmark

response (BMR) for continuous endpoints. *Critical Reviews in Toxicology* 47:342-351.

Slob W, Setzer RW. 2014. Shape and Steepness of Toxicological Dose–response Relationships

of Continuous Endpoints. *Critical Reviews in Toxicology* 44:270–97.

Soeteman-Hernández LG, Fellows MD, Johnson GE, Slob W. 2015. Correlation of in vivo

versus in vitro benchmark doses (BMDs) derived from micronucleus test data: Proof of

concept study. *Toxicol Sci* 148:355-367.

Soeteman-Hernández LG, Johnson GE, Slob W. 2016. Estimating the carcinogenic potency of chemicals from the in vivo micronucleus test. *Mutagenesis* 31:347-58.

Sprycel® (dasatinib) [package insert] Bristol-Myers Squibb Co, Princeton, NJ. (2010). Available at: [https://www.accessdata.fda.gov/drugsatfda\\_docs/label/2010/021986s7s8lbl.pdf](https://www.accessdata.fda.gov/drugsatfda_docs/label/2010/021986s7s8lbl.pdf).

Accessed October 12, 2018.

Storer RD, McKelvey TW, Kraynaka AR, Elia MC, Barnum JE, Harmon LS, Nichols WW, DeLuca JG. 1996. Revalidation of the in vitro alkaline elution/hepatocyte assay for DNA damage: improved criteria for assessment of cytotoxicity and genotoxicity and results for 81 compounds. *Mutat Res* 368:59-101.

Tagrisso™ (Osimertinib) [package insert] AstraZeneca Pharmaceuticals LP, Wilmington, DE.

2012. Available at:

[https://www.accessdata.fda.gov/drugsatfda\\_docs/label/2015/208065s000lbl.pdf](https://www.accessdata.fda.gov/drugsatfda_docs/label/2015/208065s000lbl.pdf).

Accessed October 12, 2018.

Tayama S, Nakagawa Y. 2001. Cytogenetic effects of propyl gallate in CHO-K1 cells. *Mutat Res* 498:117-127.

Tweats DJ, Johnson GE, Scandale I, Whitwell J, Evans DB. 2016. Genotoxicity of flubendazole and its metabolites in vitro and the impact of a new formulation on in vivo aneugenicity. *Mutagenesis* 31:309-321.

Van Hummelen P, Elhajouji A, Kirsch-Volders M. 1995. Clastogenic and aneugenic effects of three benzimidazole derivatives in the in vitro micronucleus test using human lymphocytes. *Mutagenesis* 10:23-29.

Verdoodt B, Decordier I, Geleyns K, Cunha M, Cundari E, Kirsch-Volders M. 1999. Induction of polyploidy and apoptosis after exposure to high concentrations of the spindle poison nocodazole.

Wills JW, Johnson GE, Doak SH, Soeteman-Hernández LG, Slob W, White PA. 2015. Empirical



Analysis of BMD Metrics in Genetic Toxicology Part I: In Vitro Analyses to Provide Robust Potency Rankings and Support MOA Determinations. *Mutagenesis* 31:255-263.

Youngblom JH, Wiencke JK, Wolff S. 1989. Inhibition of the adaptive response of human lymphocytes to very low doses of ionizing radiation by the protein synthesis inhibitor cycloheximide. *Mutat Res* 227:257-261.

Zeller A, Tang L, Dertinger SD, Funk J, Duran-Pacheco G, Guerard M. 2016. A proposal for a novel rationale for critical effect size in dose-response analysis based on a multi-endpoint in vivo study with methyl methanesulfonate. *Mutagenesis* 31:239-253.

Zeller A, Duran-Pacheco G, Guerard M. 2017. An appraisal of critical effect sizes for the benchmark dose response approach to assess dose-response relationships in genetic toxicology. *Archives of Toxicology* 91:3799-3807.

Zerit [packet insert] Bristol-Myers Squibb Virology, Princeton, NJ, 2002.

[http://www.accessdata.fda.gov/drugsatfda\\_docs/label/2002/20412S017.pdf](http://www.accessdata.fda.gov/drugsatfda_docs/label/2002/20412S017.pdf). Accessed October 12, 2018.

## FIGURE LEGENDS

**Figure 1.** Flow chart representing a tiered MultiFlow assay data analysis pipeline. With this strategy chemicals are evaluated for their genotoxic potential and genotoxic mode of action (tier 1), insights into molecular target are provided by unsupervised clustering (tier 2), and finally potency metrics are generated (tier 3).

**Figure 2.** Radar plots show MultiFlow assay data for seven biomarker/time point combinations and for each of four chemicals: thapsigargin, 4-nitroquinoline 1-oxide (4NQO), mebendazole, and crizotinib. The biomarker data are expressed as fold-increase over mean solvent control on the same plate, and each chemical concentration appears as a different colored line. The top-most endpoint (24 hr p53, at 12 o'clock) is a pan-genotoxic biomarker, whereas the biomarkers arranged on the right side of the graph are responsive to clastogens and those arranged on the left are responsive to aneugens.

**Figure 3.** Radar plots show MultiFlow assay data for seven biomarker/time point combinations and for each of two chemicals: MSD-supplied test compounds 13m and 16p. The biomarker data are expressed as fold-increase over mean solvent control on the same plate, and each chemical concentration appears as a different colored line. Same format as Figure 2.

**Figure 4.** Unsupervised clustering results are shown as a two dimensional dendrogram for 21 chemicals that were identified as exhibiting aneugenic activity. As described in Materials and Methods, each biomarker dose response was converted to an area under the curve for this analysis. The abbreviations TB (tubulin binder) and KI (kinase inhibitor) are used to denote clades with chemicals that are known to exhibit these activities. The bottom-most graph shows the horizontal distances between join points.

**Figure 5.** Unsupervised clustering results are shown as a two dimensional dendrogram for 46 chemicals that were identified as exhibiting clastogenic activity. As described in Materials and Methods, each biomarker dose response was converted to an area under the curve for this analysis. The abbreviations TI (topoisomerase inhibitor) and C-L (cross-linker) are used to denote clades that are enriched for chemicals known to exhibit these activities. The bottom-most graph shows the horizontal distances between join points.

**Figure 6.** Left panel: BMD analyses of aneugen compounds represented in cross system plots with BMD50 CIs for *in vitro* MN against BMD50 CIs 24 hr p-H3 responses in TK6 cells, with both x and y axes representing Log10 concentration of compounds in  $\mu\text{M}$ . The dashed parallel lines are drawn in such a way that encompasses most of the CIs. Dashed square box default PROAST output encompassing finite BMD CIs. Compound 'car' falls outside the trend with unbound CI in the 24 hr p-H3 endpoint. Right panel: BMD50 CIs for *in vitro* MN against BMD50 24 hr p53 responses in TK6 cells, with both x and y axes representing Log10 concentration of compounds in  $\mu\text{M}$ . Dashed parallel lines encompassing most of the BMD CIs, similarly to the left panel correlation plot. Dashed square box default PROAST output encompassing finite BMD CIs. Compounds 'gli' and 'des' lie outside the general observed trend, with unbound upper CI in the 24 hr p53 endpoint. Dashed horizontal lines obtain the uncertainty range with corresponding circles intercept with the x axis predicting the BMD50 for *in vitro* MN response. See Table I for compound abbreviations. Abbreviation: BMD = Benchmark Dose, CI = Confidence Interval, MN = micronucleus.

**Figure 7.** Left Panel: BMD analyses of clastogen compounds represented in cross system plots with BMD50 CIs for *in vitro* MN versus BMD50 CIs 24hr  $\gamma\text{H2AX}$  responses in TK6 cells, with both x and y axes representing Log10 concentration of compounds in  $\mu\text{M}$ . The dashed parallel

lines are drawn in such a way that encompasses all of the CIs. Dashed square box default PROAST output encompassing finite BMD CIs. Right Panel: BMD50 CIs for *in vitro* MN versus BMD50 24hr p53 responses in TK6 cells, with both x and y axes representing Log10 concentration of compounds in  $\mu\text{M}$ . Dashed parallel lines encompassing most of the BMD CIs. Dashed square box default PROAST output encompassing finite BMD CIs except outliers. Compound ola lies outside the general observed trend, with an unbound upper CI in the p53 endpoint. Compound cis displays an unbound upper CI in the p53 endpoint. See Table I for compound abbreviations. Abbreviation: BMD = Benchmark Dose, CI = Confidence Interval, MN = micronucleus.

**Figure 8.** Left Panel: BMD analyses of clastogen compounds represented in cross system plots with BMD100 CIs for *in vitro* MN versus BMD50 24hr  $\gamma\text{H2AX}$  responses in TK6 cells, with both x and y axes representing Log10 concentration of compounds in  $\mu\text{M}$ . The dashed parallel lines are drawn in such a way that encompasses all of the CIs. Dashed square box default PROAST output encompassing finite BMD CIs. Right Panel: BMD100 CIs for *in vitro* MN versus BMD50 24hr p53 responses in TK6 cells, with both x and y axes representing Log10 concentration of compounds in  $\mu\text{M}$ . Dashed parallel lines encompassing most of the BMD CIs. Dashed square box default PROAST output encompassing finite BMD CIs. See Table 1 for compound abbreviations. Abbreviation: BMD = Benchmark Dose, CI = Confidence Interval, MN = micronucleus.

**Table I.** Chemicals and *a priori* Classifications.

<b>Chemical, Abbreviation</b>	<b>CAS No., Source if not Sigma-Aldrich</b>	<b>Chemical Set</b>	<b><i>a priori</i> Mammalian Cell Genotoxicity &amp; MoA Classifications</b>	<b>Notes; References</b>
17 $\beta$ -Estradiol (est)	50-28-2	Training	Genotoxic; Aneugen	Steroid hormone; Hernández et al., 2013
AMG-900 (amg)	945595-80-2	Training	Genotoxic; Aneugen	Pan-Aurora kinase inhibitor (A/B/C); Payton et al., 2010
Carbendazim (car)	10605-21-7	Training	Genotoxic; Aneugen	Mitotic spindle poison; Van Hummelen et al., 1995
Colchicine (col)	64-86-8	Training	Genotoxic; Aneugen	Mitotic spindle poison; Kirkland et al., 2016
Crizotinib	877399-52-5	Training	Genotoxic; Aneugen	Tyrosine kinase inhibitor, potent activity against c-Met and ALK, with evidence of off-target Aurora kinase inhibition [Kong et al., 2018]
Diethylstilbestrol (des)	56-53-1	Training	Genotoxic; Aneugen	Synthetic estrogen; Parry et al., 2002
Flubendazole (flu)	31430-15-6	Training	Genotoxic; Aneugen	Mitotic spindle poison; Tweats et al., 2016
Griseofulvin (gli)	126-07-8	Training	Genotoxic; Aneugen	Mitotic spindle poison; Oliver et al., 2006
Mebendazole (meb)	31431-39-7	Training	Genotoxic; Aneugen	Mitotic spindle poison; Van Hummelen et al., 1995
Nocodazole (noc)	31430-18-9	Training	Genotoxic; Aneugen	Mitotic spindle poison; Verdoodt et al., 1999
Noscapine (nos)	128-62-1	Training	Genotoxic; Aneugen	Mitotic spindle poison; Schuler et al., 1999
Paclitaxel (pac)	33069-62-4	Training	Genotoxic; Aneugen	Mitotic spindle poison; Kirkland et al., 2016
Vinblastine sulfate (vin)	143-67-9	Training	Genotoxic; Aneugen	Mitotic spindle poison; Kirkland et al., 2016
Vincristine sulfate (vis)	2068-78-2	Training	Genotoxic; Aneugen	Mitotic spindle poison; Kondo et al., 1992

1,3-Propane sultone (psu)	1120-71-4	Training	Genotoxic; Clastogen	Alkylator; Dertinger et al., 2011
4-Nitroquinoline 1-oxide (nqo)	56-57-5	Training	Genotoxic; Clastogen	Likely several modes of clastogenic action that may include ROS; Kirkland et al., 2016
5-Fluorouracil	51-21-8	Training	Genotoxic; Clastogen	Anti-metabolite, thymidylate synthase inhibitor; Kirkland et al., 2016
Aphidicolin	38966-21-1	Training	Genotoxic; Clastogen	DNA polymerase inhibitor; Glover et al., 1984
Azathioprine	446-86-6	Training	Genotoxic; Clastogen	Prodrug of mercaptopurine, purine analog; Henderson et al., 1993
Azidothymidine (azt)	30516-87-1	Training	Genotoxic; Clastogen	Nucleoside analog; Kirkland et al., 2016
Bleomycin sulfate (bls)	9041-93-4	Training	Genotoxic; Clastogen	Radiomimetic; Rosefort et al., 2004
Camptothecin (cam)	7689-03-4	Training	Genotoxic; Clastogen	Topoisomerase I inhibitor; Attia et al., 2009
Chlorambucil (chl)	305-03-3	Training	Genotoxic; Clastogen	Nitrogen mustard-type alkylator; Dertinger et al., 2012
Cisplatin (cis)	15663-27-1	Training	Genotoxic; Clastogen	Atypical alkylator; Kirkland et al., 2016
Cytosine arabinoside (cya)	147-94-4	Training	Genotoxic; Clastogen	Anti-metabolite; Kirkland et al., 2016
Doxorubicin	23214-92-8	Training	Genotoxic; Clastogen	Anthracycline, likely several modes of action that includes inhibition of topoisomerase II; Gewirtz DA, 1999
Emodin	518-82-1	Training	Genotoxic; Clastogen	Anthraquinone, topoisomerase II inhibitor; Li et al., 2010
Ethyl methanesulfonate (ems)	62-50-0	Training	Genotoxic; Clastogen	Alkylator; Gocke et al., 2009
Etoposide (etp)	33419-42-0	Training	Genotoxic; Clastogen	Topoisomerase II inhibitor; Kirkland et al., 2016

Glycidamide (gly)	5694-00-8	Training	Genotoxic; Clastogen	Major in vivo metabolite of acrylamide; Paulsson et al., 2003
Hydralazine HCl	304-20-1	Training	Genotoxic; Clastogen	Prepared in RPMI medium; Martelli et al., 1995
Hydrogen peroxide (hyp)	7722-84-1	Training	Genotoxic; Clastogen	ROS, prepared in RPMI medium; Kimura et al., 2013
Hydroxyurea (hyu)	127-07-1	Training	Genotoxic; Clastogen	Anti-metabolite, ribonucleotide reductase inhibitor; Dertinger et al., 2012
Melphalan	142-82-3	Training	Genotoxic; Clastogen	Nitrogen mustard-type alkylator; Dertinger et al., 2012
Menadione (men)	58-27-5	Training	Genotoxic; Clastogen	ROS implicated; Cojocel et al., 2006
Methotrexate	59-05-2	Training	Genotoxic; Clastogen	Anti-metabolite; Keshava et al., 1998
Methyl methanesulfonate	66-27-3	Training	Genotoxic; Clastogen	Alkylator; Kirkland et al., 2016
N-Methyl-N'-nitro-N-nitrosoguanidine (MNNG)	70-25-7	Training	Genotoxic; Clastogen	Alkylator; Nikolova et al., 2014
Mitomycin C (mmc)	50-07-7	Training	Genotoxic; Clastogen	DNA cross-linker; Kirkland et al., 2016
N-Ethyl-N-nitrosourea	759-73-9	Training	Genotoxic; Clastogen	Alkylator; Kirkland et al., 2016
Olaparib (ola)	763113-22-0	Training	Genotoxic; Clastogen	PARP inhibitor; FDA approved label (Lynparza™)
Propyl gallate	121-79-9	Training	Genotoxic; Clastogen	ROS likely; Tayama and Nakagawa, 2001
Resorcinol diglycidyl ether	101-90-6	Training	Genotoxic; Clastogen	Gulati et al., 1989
Stavudine	3056-17-5	Training	Genotoxic; Clastogen	Nucleoside analog; FDA approved label (Zerit®)
Temozolomide (tmz)	85622-93-1	Training	Genotoxic; Clastogen	Alkylator; Chinnasamy et al., 1997

Thiotepe (thi)	52-24-4	Training	Genotoxic; Clastogen	Alkylator; Dertinger et al., 2012
Topotecan (top)	123948-87-8	Training	Genotoxic; Clastogen	Topoisomerase I inhibitor; Aydemir and Bilaloğlu, 2003
Alosetron HCl	122852-42-0	Training	Non-genotoxic	5-HT <sub>3</sub> antagonist; Kirkland et al., 2016
Amitrole	61-82-5	Training	Non-genotoxic	Kirkland et al., 2016
Anthranilic acid	118-92-3	Training	Non-genotoxic	Kirkland et al., 2016
Brefeldin A	20350-15-6	Training	Non-genotoxic	ER-golgi transporter inhibitor, ER stress-induced apoptosis; Moon et al., 2012
Caffeine	58-08-2	Training	Non-genotoxic	Mitochondria-dependent apoptosis, ROS involvement likely; Lu et al., 2008
Carbonyl cyanide m-chlorophenyl hydrazone (CCCP)	555-60-2	Training	Non-genotoxic	Uncoupler of oxidative phosphorylation; de Graaf et al., 2004
Clofibrate	637-07-0	Training	Non-genotoxic	Antilipidemic agent; IARC monograph
Cyclohexanone	108-94-1	Training	Non-genotoxic	Industrial chemical; Kirkland et al., 2008
Cycloheximide	66-81-9	Training	Non-genotoxic	Protein synthesis inhibitor; Youngblom et al., 1989
D-Limonene	5989-27-5	Training	Non-genotoxic	Male rat kidney tumors due to $\alpha$ 2 $\mu$ -globulin nephropathy; Kirkland et al., 2016
D-Mannitol	69-65-8	Training	Non-genotoxic	Polyol; Kirkland et al., 2016
Dexamethasone	50-02-2	Training	Non-genotoxic	Glucocorticoid receptor agonist; Krishna et al., 1995
Dextrose	50-99-7	Training	Non-genotoxic	Sugar; Lotz et al., 2009
Di-(2-ethylhexyl)phthalate (DEHP)	117-81-7	Training	Non-genotoxic	Organic plasticizer; Kirkland et al., 2016
Diethanolamine	111-42-2	Training	Non-genotoxic	Secondary amine; Kirkland et al., 2016
Erythromycin	114-07-8	Training	Non-genotoxic	Antibiotic; Kirkland et al., 2016



Famotidine	76824-35-6	Training	Non-genotoxic	Histamine H <sub>2</sub> receptor antagonist; FDA approved label (Pepcid <sup>®</sup> )
Imatinib mesylate	152459-95-5	Training	Non-genotoxic	Protein-tyrosine kinase inhibitor; FDA approved label (Gleevec <sup>®</sup> )
Hexachloroethane	67-72-1	Training	Non-genotoxic	Industrial chemical; Kirkland et al., 2016
Lidocaine	137-58-6	Training	Non-genotoxic	Amide, local anesthetic; FDA approved label (Lidoderm <sup>®</sup> )
Lovastatin	75330-75-5	Training	Non-genotoxic	HMG-CoA reductase inhibitor; FDA approved label (Mevacor <sup>®</sup> )
Melamine	108-78-1	Training	Non-genotoxic	Industrial organic base; Kirkland et al., 2016
Methyl carbamate	598-55-0	Training	Non-genotoxic	Industrial intermediate; Kirkland et al., 2016
<i>N</i> -Butyl chloride	109-69-3	Training	Non-genotoxic	Fumigant; Kirkland et al., 2016
Ofloxacin	82419-36-1	Training	Non-genotoxic	Fluoroquinolone antibiotic; FDA approved label (Floxin <sup>®</sup> )
Paroxetine	61869-08-7	Training	Non-genotoxic	SSRI antidepressant; FDA approved label (Paxil <sup>®</sup> )
Phenanthrene	85-01-8	Training	Non-genotoxic	Polycyclic aromatic hydrocarbon; Kirkland et al., 2008
Phenformin HCl	834-28-6	Training	Non-genotoxic	Biguanide antidiabetic; Kirkland et al., 2016
Progesterone	57-83-0	Training	Non-genotoxic	Steroid hormone; Kirkland et al., 2008
Pyridine	110-86-1	Training	Non-genotoxic	Heterocyclic organic compound; Kirkland et al., 2016
Sodium chloride	7647-14-5	Training	Non-genotoxic	Prepared in RPMI medium; Matsushima et al., 1999
Sodium dodecyl sulfate	151-21-3	Training	Non-genotoxic	Ionic detergent; NTP database
Sucrose	57-50-1	Training	Non-genotoxic	Diaz et al., 2007

Tert-butyl alcohol	75-65-0	Training	Non-genotoxic	Kirkland et al., 2016
Thapsigargin	67526-95-8	Training	Non-genotoxic	ER stress-induced apoptosis; Futami et al., 2005
Tolterodine L-tartrate	124937-52-6	Training	Non-genotoxic	Muscarinic receptor antagonist; Kirkland et al., 2016
Tunicamycin	11089-65-9	Training	Non-genotoxic	Glycosylation inhibitor, ER stress-mediated apoptosis; Han et al., 2008
Zonisamide	68291-97-4	Training	Non-genotoxic	Sulfonamide anticonvulsant; Kirkland et al., 2016
10j	MSD	Test	Genotoxic; Aneugen	Tyrosine kinase inhibitor; Ames neg., CHO MN pos., CHO ChromAb neg. but polyploidy evident; MSD in-house results
13m	MSD	Test	Genotoxic; assumed Aneugen	Tyrosine kinase inhibitor; CHO and TK6 MN pos.; MSD in-house results
14n	MSD	Test	Genotoxic; Aneugen	Serine/threonine kinase inhibitor; Ames neg., CHO MN pos., CHO ChromAb neg. but polyploidy and endoreduplication evident; TK6 MN neg.; MSD in-house results
16p	MSD	Test	Genotoxic; Mixed	Azobenzimidazole structure; Likely >1 MoA; Ames neg., CHO MN and ChromAb pos. with premature centromere separation at metaphase in addition to structural aberrations, Rat MN neg.; MSD in-house results
17q	MSD	Test	Genotoxic; assumed Aneugen	Benzimidazole structure; Ames neg., CHO MN pos.; MSD in-house results

Phenolphthalein, supplied coded as 3c	77-09-8; MSD	Test	Genotoxic; Mixed	Likely >1 MoA; Spindle poison, centromere amplification [Heard et al., 2013]; CHO ChromAb pos.; MSD in-house results
6f	MSD	Test	Genotoxic; Aneugen	Kinase inhibitor, leucine-rich repeat; Ames neg., CHO MN pos., CHO ChromAb neg., rat MN pos.; MSD in-house results
Hesperadin	422513-13-1; Selleckchem	Test	Genotoxic; Aneugen	Aurora kinase inhibitor (B); in vitro MN pos., aberrant metaphases; Hauf et al., 2003; Kurihara et al., 2006
Tozasertib	639089-54-6; Selleckchem	Test	Genotoxic; Aneugen	Pan-Aurora kinase inhibitor (A/B/C); Gollapudi et al., 2014
ZM-447439	331771-20-1; Selleckchem	Test	Genotoxic; Aneugen	Aurora kinase inhibitor (A/B); Gollapudi et al., 2014
7g	MSD	Test	Genotoxic, MoA uncertain	Possibly > 1 MoA; Ames pos., CHO MN pos., CHO ChromAb neg., TK6 MN pos., HPBL MN neg.; mechanism affects tubulin so suspected aneugen, but Ames pos. suggests primary DNA damage; MSD in-house results
9i	MSD	Test	Genotoxic; Clastogen	Non-nucleoside antiviral; Ames neg., CHO MN pos., CHO ChromAb pos.; MSD in-house results
AZD2858	486424-20-8; Selleckchem	Test	Genotoxic; Clastogen	Glycogen synthase-3 inhibitor; in vitro MN and ChromAb pos., Ann Doherty, personal communication
Beta-Lapachone	4707-32-8; Selleckchem	Test	Genotoxic; Clastogen	Topoisomerase I inhibitor; in vitro ChromAb and comet pos.; Degradi et al. 1993

Ciprofloxacin	85721-33-1; Selleckchem	Test	Genotoxic; Clastogen	Topoisomerase II inhibitor; in vitro MN pos.; Curry et al. 1996
Dasatinib	302962-49-8; Selleckchem	Test	Genotoxic; Clastogen	Tyrosine kinase inhibitor, especially Ber-Abl, Scr, c-Kit; Ames neg., clastogenic in CHO, in vivo MN neg.; Sprycel package insert, 2010
Genistein	446-72-0	Test	Genotoxic; Clastogen	Topoisomerase II inhibitor; in vitro MN pos.; Klein and King, 2007
Irinotecan	57852-57-0; Selleckchem	Test	Genotoxic; Clastogen	Topoisomerase I inhibitor; Ames neg., in vitro ChromAb pos., in vivo MN pos.; Camptosar packet insert, 2014
Mitoxantrone 2HCl	70476-82-3; Selleckchem	Test	Genotoxic; Clastogen	Topoisomerase II inhibitor; in vitro MN pos., $\gamma$ H2AX pos.; Smart et al. 2008
Teniposide	29767-20-2; Selleckchem	Test	Genotoxic; Clastogen	Topoisomerase II inhibitor; in vitro ChromAb pos., in vitro MLA pos.; DeMarini et al. 1987
Entecavir, supplied coded as 19s	MSD	Test	Genotoxic; Clastogen	Guanine nucleoside analog; CHO MN pos., CHO ChromAb pos.; MSD in-house data
Hydroquinone, supplied coded as 1a	123-31-9; MSD	Test	Genotoxic; Mixed	Likely >1 MoA; Kirkland et al., 2016
20t	MSD	Test	Genotoxic; Clastogen	Adenosine nucleoside analog; Ames neg., CHO MN pos., CHO ChromAb pos.; MSD in-house results
Tetrahydroxydiboron, supplied coded as 4d	MSD	Test	Genotoxic; Clastogen	Ames pos., CHO MN pos., CHO ChromAb pos.; MSD in-house results
6-Thioguanine	154-42-7	Test	Genotoxic; Clastogen	Antimetabolite, purine analog; Ames pos., in vitro ChromAb pos., in vivo MN pos.; NTP

				database
11k	MSD	Test	Non-genotoxic	Tyrosine kinase inhibitor; Ames neg., CHO MN neg., Rat MN neg.; MSD in-house data
12L	MSD	Test	Non-genotoxic	Drug candidate; Ames neg., CHO MN neg.; MSD in-house results
15o	MSD	Test	Non-genotoxic (in TK6 cells)	Tyrosine kinase inhibitor; CHO MN weak pos. only at 24 hr; CHO ChromAb neg., TK6 MN neg., Rat MN neg.; MSD in-house results
18r	MSD	Test	Non-genotoxic	Benzimidazole structure; Ames neg., CHO MN neg.; MSD in-house results
2b	20624-25-3; MSD	Test	Non-genotoxic	Sodium diethyldicarbamate trihydrate; CHO MN pos., TK6 MN pos., but cited authors attribute results to cytotoxicity, Hilliard et al., 1998; Galloway et al., 1998; Greenwood et al., 2004; Cu and Zn chelator, superoxide dismutase inhibitor, Heikkila et al. 1976; Nicotera et al. 1989
5e	MSD	Test	Non-genotoxic (in mammalian cells)	Aryl boronic acid; Ames pos., CHO MN neg.; MSD in-house results
8h	MSD	Test	Non-genotoxic	HDAC inhibitor; Ames neg., CHO MN neg.; CHO ChromAb neg.; MSD in-house results
Ampicillin trihydrate	7177-48-2	Test	Non-genotoxic	Ames neg., in vitro ChromAb neg., in vivo MN neg.; Kirkland et al., 2016
Anisomycin	22862-76-6	Test	Non-genotoxic	Protein biosynthesis inhibitor; in vitro MN neg. with high levels of apoptosis; personal

				communication, Maik Schuler
Chlorocholine chloride	999-81-5	Test	Non-genotoxic	Ames neg., in vitro and in vivo ChromAb neg.; Kirkland et al., 2016
Menthol	89-78-1	Test	Non-genotoxic	Ames neg., in vitro MN neg. in p53 competent cell lines, in vivo MN and comet neg.; Kirkland et al., 2016
Osimertinib	1421373-65-0	Test	Non-genotoxic	EGFR kinase inhibitor; in vitro and in vivo genotox neg.; Tagrisso package insert, 2012
Topiramate	97240-79-4	Test	Non-genotoxic	Ames, in vitro ChromAb and MLA neg., in vivo ChromAb Neg.; Kirkland et al., 2016
Tris (2-ethylhexyl) phosphate	78-42-2	Test	Non-genotoxic	Ames neg., in vitro ChromAb neg., in vivo ChromAb and MN neg.; Kirkland et al., 2016
Zafirlukast	107753-78-6	Test	Non-genotoxic	Ames, in vitro ChromAb, MLA, and Hprt neg.; Kirkland et al., 2016

Abbreviations: MDS = Merck Sharp & Dohme Corp., a subsidiary of Merck & Co., Inc.;

FDA = US Food and Drug Administration; NTP = National Toxicology Program; PARP = poly ADP ribose polymerase; ROS = reactive oxygen species; MN = micronuclei;

ChromAb = chromosome aberration; MLA = mouse lymphoma assay; ER =

endoplasmic reticulum; Hprt = hypoxanthine guanine phosphoribosyltransferase; EGFR

= epithelial growth factor receptor; MoA = mode of action; CHO = Chinese hamster ovary cells

Table II. Training Set Chemicals, N = 85

Chemical	Group	a priori Genotox Expectation	Machine Learning (ML) Ensemble						Global Evaluation Factor (GEF) Rubric				ML + GEF			
			Aneugen Calls			Clastogen Calls			Overall ML Genotoxicity Call	Overall ML MoA Call	Aneugen Calls	Clastogen Calls	Overall GEF Genotoxicity Calls	Overall GEF MoA Calls	Overall ML + GEF Genotoxicity Calls	Overall ML + GEF MoA Calls
			RF	LR	ANN	RF	LR	ANN								
17 $\beta$ -Estradiol	Training	Aneugen	+	+	+	-	-	-	+	A	+	-	+	A	+	A
AMG-900	Training	Aneugen	+	+	+	-	-	-	+	A	+	-	+	A	+	A
Carbendazim	Training	Aneugen	+	+	+	-	-	-	+	A	+	-	+	A	+	A
Colchicine	Training	Aneugen	+	+	+	-	-	-	+	A	+	-	+	A	+	A
Crizotinib	Training	Aneugen	+	+	+	-	-	-	+	A	+	-	+	A	+	A
Diethylstilbestrol	Training	Aneugen	+	+	+	-	-	-	+	A	+	-	+	A	+	A
Flubendazole	Training	Aneugen	+	+	+	-	-	-	+	A	+	-	+	A	+	A
Griseofulvin	Training	Aneugen	+	+	+	-	-	-	+	A	+	-	+	A	+	A
Mebendazole	Training	Aneugen	+	+	+	-	-	-	+	A	+	-	+	A	+	A
Nocodazole	Training	Aneugen	+	+	+	-	-	-	+	A	+	-	+	A	+	A
Noscapine	Training	Aneugen	+	+	+	-	-	-	+	A	+	-	+	A	+	A
Paclitaxel	Training	Aneugen	+	+	+	-	-	-	+	A	+	-	+	A	+	A
Vinblastine sulfate	Training	Aneugen	+	+	+	-	-	-	+	A	+	-	+	A	+	A
Vincristine sulfate	Training	Aneugen	+	+	+	-	-	-	+	A	+	-	+	A	+	A
1,3-Propane sultone	Training	Clastogen	-	-	-	+	+	+	+	C	-	+	+	C	+	C
4-Nitroquinoline N-oxide	Training	Clastogen	-	-	-	+	+	+	+	C	-	+	+	C	+	C
5-Fluorouracil	Training	Clastogen	-	-	-	+	+	+	+	C	-	+	+	C	+	C
Aphidicolin	Training	Clastogen	-	-	-	+	+	+	+	C	-	+	+	C	+	C
Azathioprine	Training	Clastogen	-	-	-	+	+	+	+	C	-	-	-	-	+	C
Azidothymidine	Training	Clastogen	-	-	-	+	+	+	+	C	-	-	-	-	+	C
Bleomycin sulfate	Training	Clastogen	-	-	-	+	+	+	+	C	-	+	+	C	+	C
Camptothecin	Training	Clastogen	-	-	-	+	+	+	+	C	-	+	+	C	+	C
Carbambucil	Training	Clastogen	-	-	-	+	+	+	+	C	-	+	+	C	+	C
Cisplatin	Training	Clastogen	-	-	-	+	+	+	+	C	-	+	+	C	+	C
Cytosine Arabinoside	Training	Clastogen	-	-	-	+	+	+	+	C	-	+	+	C	+	C
Doxorubicin	Training	Clastogen	-	-	-	+	+	+	+	C	-	+	+	C	+	C
Emodin	Training	Clastogen	-	-	-	+	+	+	+	C	-	-	-	-	+	C
Ethyl methanesulfonate	Training	Clastogen	-	-	-	+	+	+	+	C	-	+	+	C	+	C
Etoposide	Training	Clastogen	-	-	-	+	+	+	+	C	-	+	+	C	+	C
Glycidamide	Training	Clastogen	-	-	-	+	+	+	+	C	-	+	+	C	+	C
Hydralazine	Training	Clastogen	-	-	-	+	+	+	+	C	-	+	+	C	+	C
Hydrogen peroxide	Training	Clastogen	-	-	-	+	+	+	+	C	-	+	+	C	+	C
Hydroxyurea	Training	Clastogen	-	-	-	+	+	+	+	C	-	+	+	C	+	C
Melphalan	Training	Clastogen	-	-	-	+	+	+	+	C	-	+	+	C	+	C
Menadione	Training	Clastogen	-	-	-	+	+	-	+	C	-	-	-	-	+	C
Methotrexate	Training	Clastogen	-	-	-	+	+	+	+	C	-	-	-	-	+	C
Methyl methanesulfonate	Training	Clastogen	-	-	-	+	+	+	+	C	-	+	+	C	+	C
Mitomycin C	Training	Clastogen	-	-	-	+	+	+	+	C	-	+	+	C	+	C
N-Ethyl-N-nitrosourea	Training	Clastogen	-	-	-	+	+	+	+	C	-	+	+	C	+	C
N-Methyl-N'-nitro-N-nitrosoguanidine	Training	Clastogen	-	-	-	+	+	+	+	C	-	+	+	C	+	C
Olaparib	Training	Clastogen	-	-	-	+	+	+	+	C	-	+	+	C	+	C
Propyl gallate	Training	Clastogen	-	-	-	+	+	+	+	C	-	+	+	C	+	C
Resorcinol diglycidyl ether	Training	Clastogen	-	-	-	+	+	+	+	C	-	+	+	C	+	C
Stavudine	Training	Clastogen	-	-	-	+	+	+	+	C	-	+	+	C	+	C
Tamoxolomide	Training	Clastogen	-	-	-	+	+	+	+	C	-	+	+	C	+	C
Tamoxifen	Training	Clastogen	-	-	-	+	+	+	+	C	-	+	+	C	+	C
Topotecan	Training	Clastogen	-	-	-	+	+	+	+	C	-	+	+	C	+	C
Alosetron	Training	Non-genotoxicant	-	-	-	-	-	-	-	-	-	-	-	-	-	-
Amitrole	Training	Non-genotoxicant	-	-	-	-	-	-	-	-	-	-	-	-	-	-
Anthranilic acid	Training	Non-genotoxicant	-	-	-	-	-	-	-	-	-	-	-	-	-	-
Brefeldin A	Training	Non-genotoxicant	-	-	-	-	-	-	-	-	-	-	-	-	-	-
Caffeine	Training	Non-genotoxicant	-	-	-	-	-	-	-	-	-	-	-	-	-	-
CCCP	Training	Non-genotoxicant	-	-	-	-	-	-	-	-	-	-	-	-	-	-
Clofibrate	Training	Non-genotoxicant	-	-	-	-	-	-	-	-	-	-	-	-	-	-
Cyclohexanone	Training	Non-genotoxicant	-	-	-	-	-	-	-	-	-	-	-	-	-	-
Cycloheximide	Training	Non-genotoxicant	-	-	-	-	-	-	-	-	-	-	-	-	-	-
D-Limonene	Training	Non-genotoxicant	-	-	-	-	-	-	-	-	-	-	-	-	-	-
D-Mannitol	Training	Non-genotoxicant	-	-	-	-	-	-	-	-	-	-	-	-	-	-
Dexamethasone	Training	Non-genotoxicant	-	-	-	-	-	-	-	-	-	-	-	-	-	-
Dextrose	Training	Non-genotoxicant	-	-	-	-	-	-	-	-	-	-	-	-	-	-
Di-(2-ethylhexyl) phthalate	Training	Non-genotoxicant	-	-	-	-	-	-	-	-	-	-	-	-	-	-
Diethanolamine	Training	Non-genotoxicant	-	-	-	-	-	+	-	-	-	-	-	-	-	-
Erythromycin	Training	Non-genotoxicant	-	-	-	-	-	-	-	-	-	-	-	-	-	-
Famotidine	Training	Non-genotoxicant	-	-	-	-	-	-	-	-	-	-	-	-	-	-
Imatinib mesylate	Training	Non-genotoxicant	-	-	-	-	+	+	+	C	-	-	-	-	+	C
Hexachloroethane	Training	Non-genotoxicant	-	-	-	-	-	-	-	-	-	-	-	-	-	-
Lidocaine	Training	Non-genotoxicant	-	-	-	-	-	-	-	-	-	-	-	-	-	-
Livastatin	Training	Non-genotoxicant	-	-	-	-	-	-	-	-	-	-	-	-	-	-
Melamine	Training	Non-genotoxicant	-	-	-	-	-	-	-	-	-	-	-	-	-	-
Methyl carbamate	Training	Non-genotoxicant	-	-	-	-	-	-	-	-	-	-	-	-	-	-
N-Butyl chloride	Training	Non-genotoxicant	-	-	-	-	-	-	-	-	-	-	-	-	-	-
Ofoxacin	Training	Non-genotoxicant	-	-	-	-	-	-	-	-	-	-	-	-	-	-
Paroxetine	Training	Non-genotoxicant	-	-	-	-	-	-	-	-	-	-	-	-	-	-
Phenanthrene	Training	Non-genotoxicant	-	-	-	-	-	-	-	-	-	-	-	-	-	-
Phenformin HCl	Training	Non-genotoxicant	-	-	-	-	-	-	-	-	-	-	-	-	-	-
Progesterone	Training	Non-genotoxicant	-	-	-	-	-	-	-	-	-	-	-	-	-	-
Pyridine	Training	Non-genotoxicant	-	-	-	-	-	-	-	-	-	-	-	-	-	-
Sodium chloride	Training	Non-genotoxicant	-	-	-	-	-	-	-	-	-	-	-	-	-	-
Sodium dodecyl sulfate	Training	Non-genotoxicant	-	-	-	-	-	-	-	-	-	-	-	-	-	-
Sucrose	Training	Non-genotoxicant	-	-	-	-	-	-	-	-	-	-	-	-	-	-
Tert-butyl alcohol	Training	Non-genotoxicant	-	-	-	-	-	-	-	-	-	-	-	-	-	-
Thapsigargin	Training	Non-genotoxicant	-	-	-	-	-	-	-	-	-	-	-	-	-	-
Toiletidine L-tartrate	Training	Non-genotoxicant	-	-	-	-	-	-	-	-	-	-	-	-	-	-
Tunicamycin	Training	Non-genotoxicant	-	-	-	-	-	-	-	-	-	-	-	-	-	-
Zonisamide	Training	Non-genotoxicant	-	-	-	-	-	-	-	-	-	-	-	-	-	-

This article is protected by copyright. All rights reserved

Concordance with a priori Expectation, Training Set:

84/85  
99%47/48  
98%79/85  
93%41/41  
100%84/85  
99%47/48  
98%

Table III. Test Set Chemicals, N = 40

Chemical	Group	<i>a priori</i> Genotox Expectation	Machine Learning (ML) Ensemble						Global Evaluation Factor (GEF) Rubric				ML + GEF			
			Aneugen Calls			Clastogen Calls			Overall ML Genotoxicity Call	Overall ML MoA Call	Aneugen Calls	Clastogen Calls	Overall GEF Genotoxicity Calls	Overall GEF MoA Calls	Overall ML + GEF Genotoxicity Calls	Overall ML + GEF MoA Calls
			RF	LR	ANN	RF	LR	ANN								
10j	Test	Aneugen	-	+	+	-	-	-	+	A	+	-	+	A	+	A
13m	Test	Aneugen	-	-	+	-	-	+	-	-	-	-	-	-	-	-
14n	Test	Aneugen	-	-	-	-	-	-	-	-	-	-	-	-	-	-
17q	Test	Aneugen	+	+	+	-	-	-	+	A	+	-	+	A	+	A
6f	Test	Aneugen	-	-	-	-	-	+	-	-	-	-	-	-	-	-
Hesperadin	Test	Aneugen	-	+	+	-	+	-	+	A	+	-	+	A	+	A
Tozasertib	Test	Aneugen	-	+	+	-	-	-	+	A	+	-	+	A	+	A
ZM-447439	Test	Aneugen	-	+	+	-	-	-	+	A	+	-	+	A	+	A
3c	Test	Aneugen, possibly >1 MoA	+	+	+	-	-	+	+	A	+	-	+	A	+	A
16p	Test	Aneugen, likely >1 MoA	+	+	+	-	+	+	+	A / C	+	-	+	A / C	+	A / C
1a	Test	Genotoxic, likely > 1 MoA	-	-	-	+	+	+	+	C	-	-	-	-	+	C
7g	Test	Genotoxic, MoA uncertain	-	-	-	+	+	+	+	C	-	-	-	-	+	C
9i	Test	Clastogen	-	-	-	+	+	+	+	C	-	-	-	-	+	C
Beta-Lapachone	Test	Clastogen	-	-	-	+	+	+	+	C	-	-	-	-	+	C
Ciprofloxacin	Test	Clastogen	-	+	+	-	-	-	+	A	-	-	-	-	+	A
Dasatinib	Test	Clastogen	-	-	-	+	+	+	+	C	-	+	+	C	+	C
Genistein	Test	Clastogen	-	-	-	+	+	+	+	C	-	+	+	C	+	C
Irinotecan	Test	Clastogen	-	-	-	+	+	+	+	C	-	+	+	C	+	C
Mitoxantrone	Test	Clastogen	-	-	+	+	+	+	+	C	-	+	+	C	+	C
Teniposide	Test	Clastogen	-	-	-	+	+	+	+	C	-	+	+	C	+	C
19s	Test	Clastogen	-	-	-	+	+	+	+	C	-	+	+	C	+	C
20t	Test	Clastogen	-	-	-	-	+	+	+	C	-	-	-	-	+	C
4d	Test	Clastogen	-	-	-	+	+	+	+	C	-	+	+	C	+	C
6-Thioguanine	Test	Clastogen	-	-	-	-	+	+	+	C	-	+	+	C	+	C
AZD2858	Test	Clastogen, possibly >1 MoA	-	-	-	+	-	+	+	C	-	-	-	-	+	C
11k	Test	Non-genotoxicant	-	-	-	-	-	-	-	-	-	-	-	-	-	-
12l	Test	Non-genotoxicant	-	-	-	+	+	+	+	C	-	+	+	C	+	C
15o	Test	Non-genotoxicant	-	-	-	-	-	-	-	-	-	-	-	-	-	-
18r	Test	Non-genotoxicant	-	-	-	-	-	-	-	-	-	-	-	-	-	-
2b	Test	Non-genotoxicant	-	-	-	+	+	+	+	C	-	-	-	-	+	C
5e	Test	Non-genotoxicant	-	-	-	-	-	-	-	-	-	-	-	-	-	-
8h	Test	Non-genotoxicant	-	-	-	-	-	+	-	-	-	-	-	-	-	-
Ampicillin	Test	Non-genotoxicant	-	-	-	-	-	-	-	-	-	-	-	-	-	-
Anisomycin	Test	Non-genotoxicant	-	-	-	-	-	-	-	-	-	-	-	-	-	-
Chlorocholine	Test	Non-genotoxicant	-	-	-	-	-	-	-	-	-	-	-	-	-	-
Menthol	Test	Non-genotoxicant	-	-	-	-	-	-	-	-	-	-	-	-	-	-
Osmertinib	Test	Non-genotoxicant	-	-	-	+	-	-	-	-	-	-	-	-	-	-
Topiramate	Test	Non-genotoxicant	-	-	-	-	-	-	-	-	-	-	-	-	-	-
Tris (2-ethylhexyl) phosphate	Test	Non-genotoxicant	-	-	-	-	-	-	-	-	-	-	-	-	-	-
Zafirlukast	Test	Non-genotoxicant	-	-	-	-	-	-	-	-	-	-	-	-	-	-
Concordance with <i>a priori</i> Expectation, Test Set:									35/40 88%	21/24 88%			30/40 75%	15/17 88%	35/40 88%	21/24 88%



Perform MultiFlow® DNA Damage Assay, Collect 4 and 24 hr Data

Calculate Fold-Change Values for Each Biomarker and Time Point  
Relative to Same-Plate Solvent Control Means

Compare Biomarker  
Responses to GEFs

Predictive Machine Learning  
(Ensemble of 3 Models)

Not Significant

Significant

Negative

Genotoxic

MoA Prediction:  
Clastogen, Aneugen, Mixed

Convert Fold-Change  
Values to AUC;  
Normalize Conc. (0-1)

Hierarchal Clustering  
Provides Insights into  
Molecular Targets

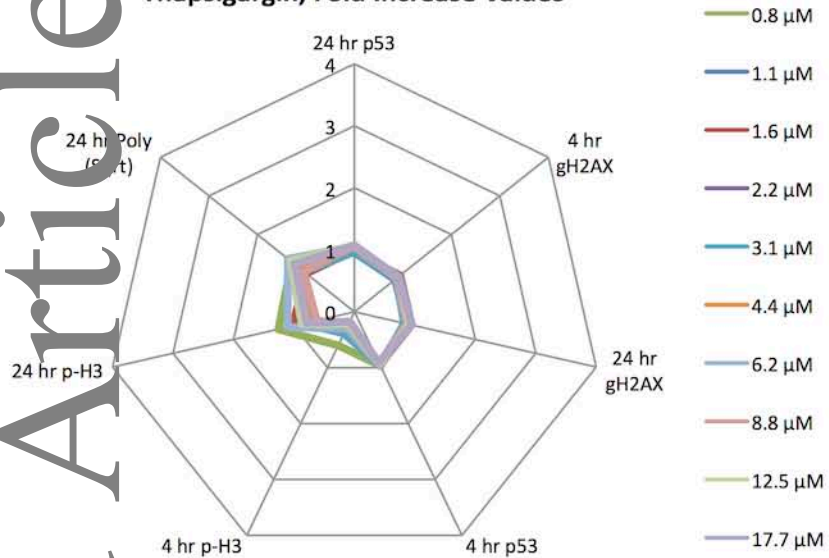
BMD Analyses Based on Biomarker  
Fold-Change Values Provide  
Potency Metrics

Tier 1 Analyses

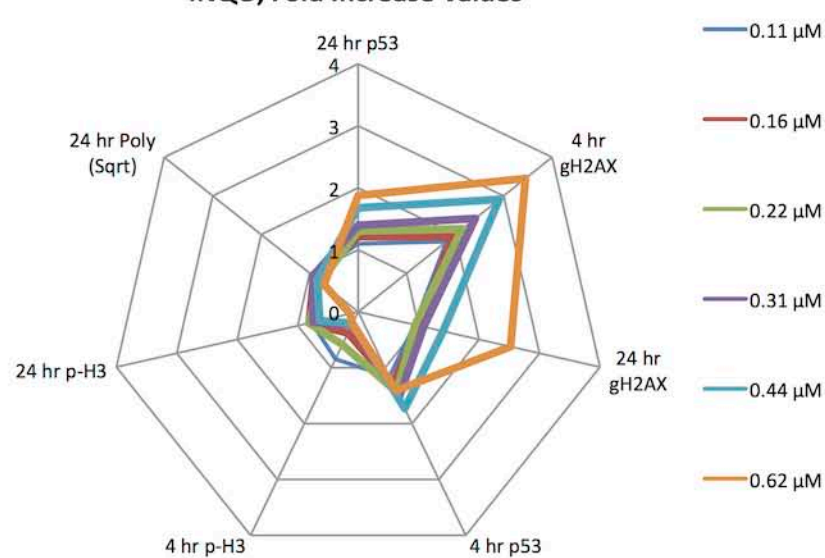
Tier 2 Analyses

Tier 3

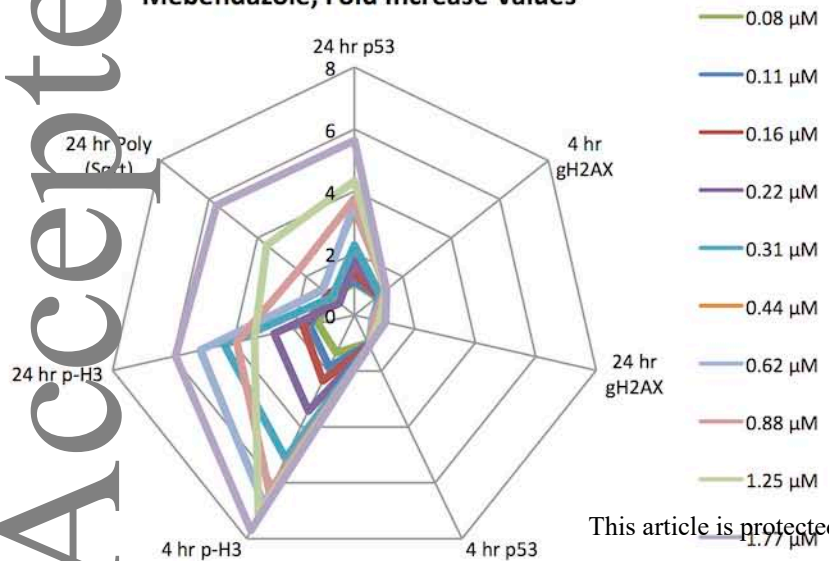
### Thapsigargin, Fold Increase Values



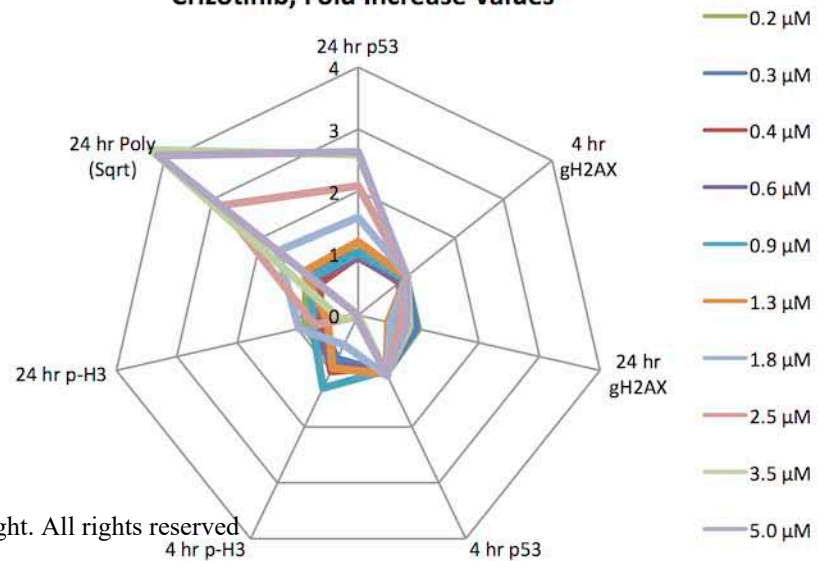
### 4NQO, Fold Increase Values



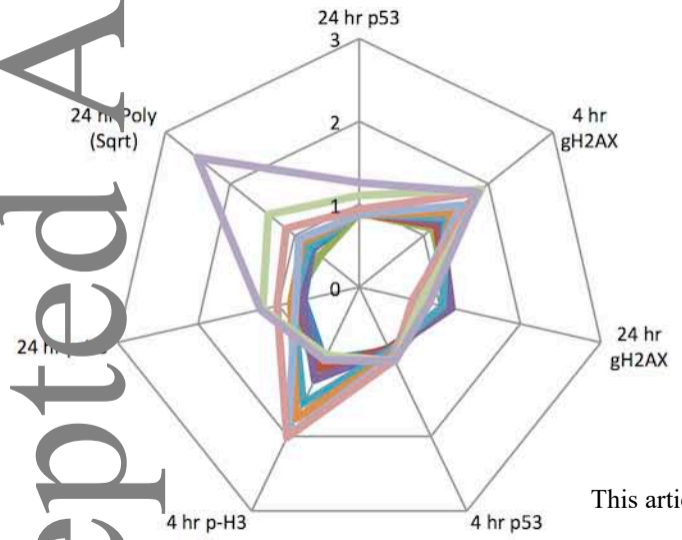
### Mebendazole, Fold Increase Values



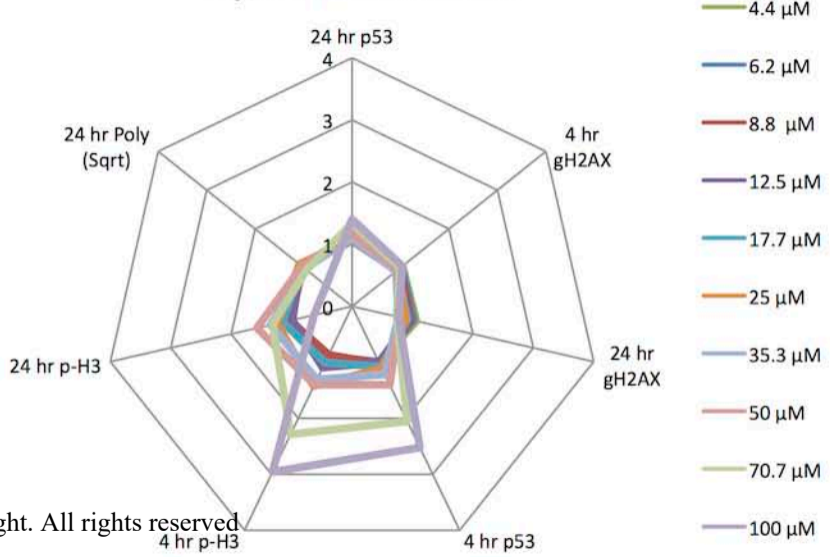
### Crizotinib, Fold Increase Values



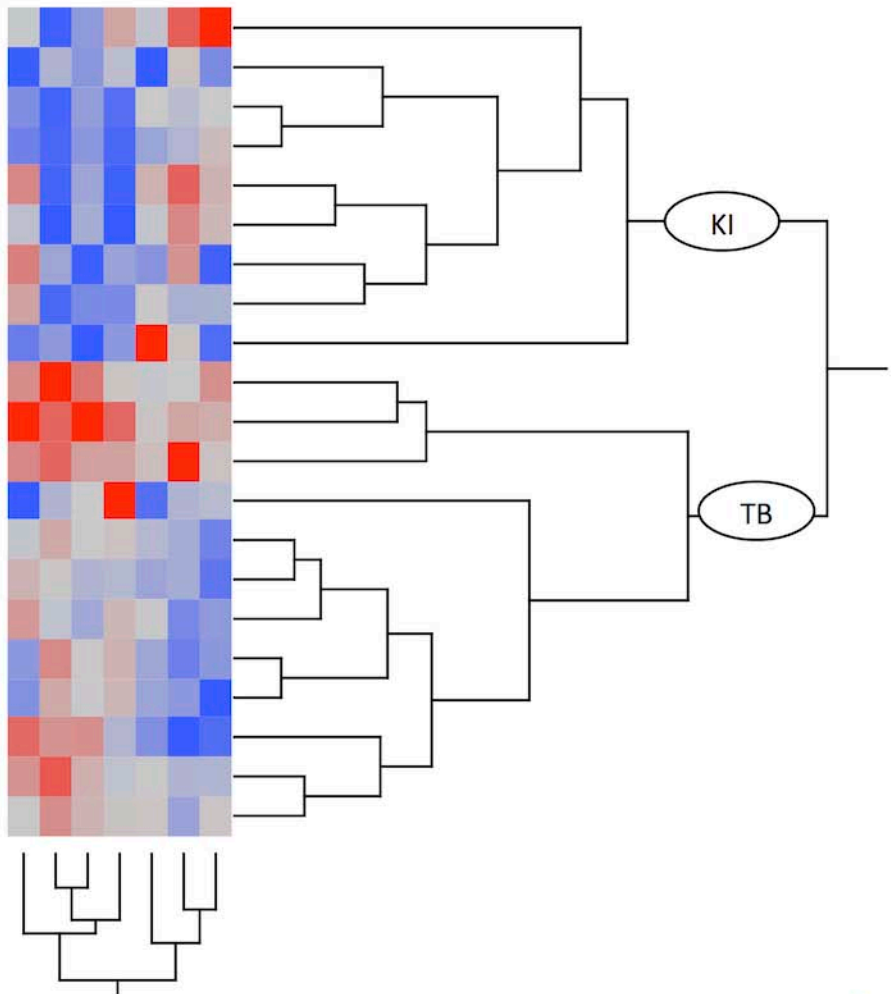
**13m, Fold Increase Values**



**16p, Fold Increase Values**



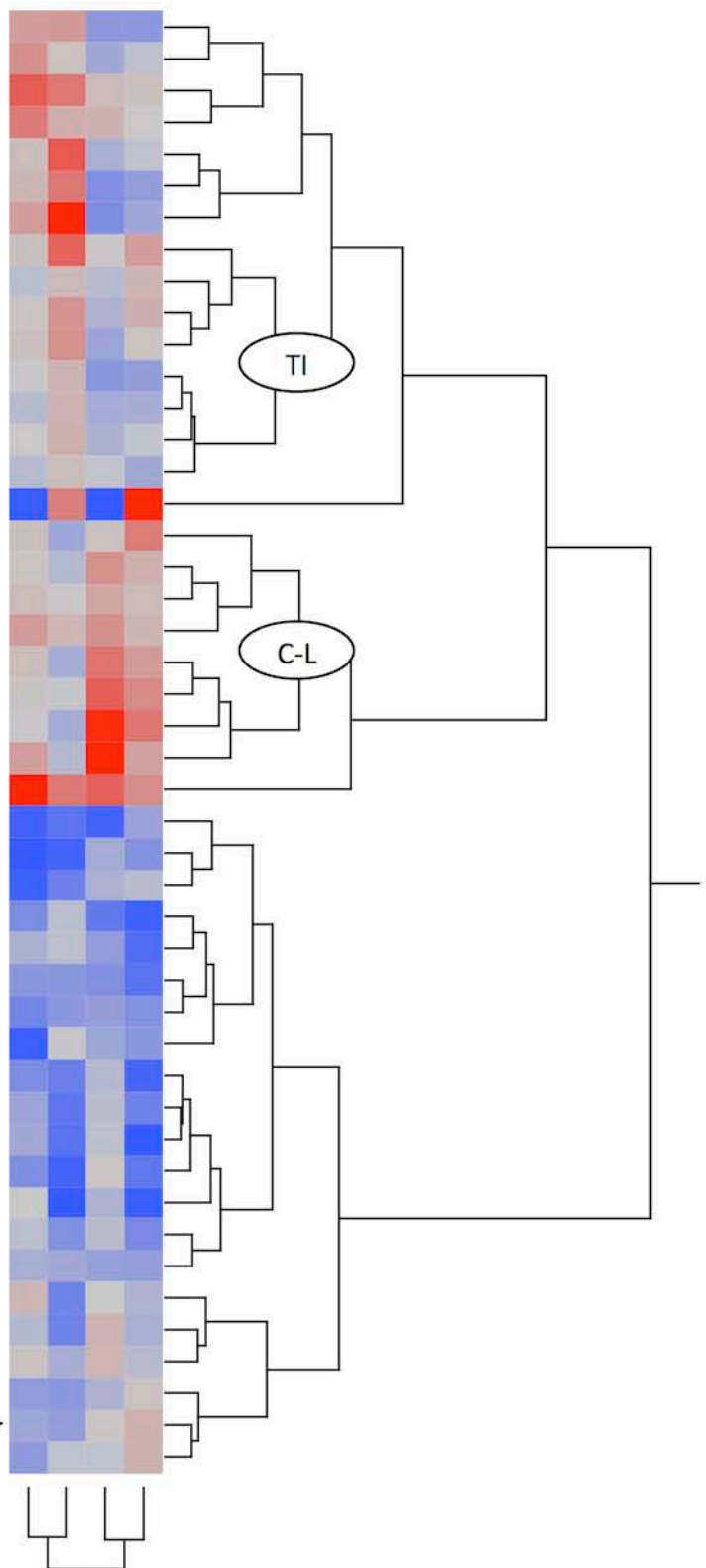
- AMG 900
- Diethylstilbestrol
- Crizotinib
- Irozasertib
- Heperadin
- ZM-141439
- 3c
- 10i
- 16p
- Carbendazim
- Mebendazole
- Paclitaxel
- Colchicine
- Griseofulvin
- 17B-Estradiol
- Nescadine
- Flubendazole
- 17q
- Nocodazole
- Vinblastine
- Vincristine sulfate



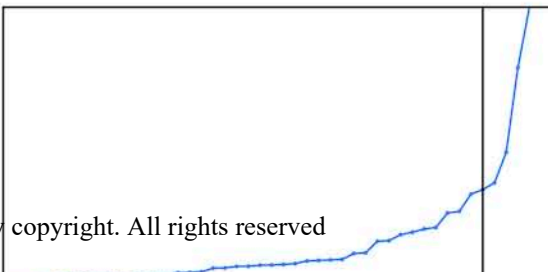
4 hr gH2AX (AUC)  
4 hr p-H3 (AUC)  
24 hr p53 (AUC)  
24 hr p-H3 (AUC)  
4 hr p53 (AUC)  
24 hr gH2AX (AUC)  
24 hr Sqrt Poly (AUC)

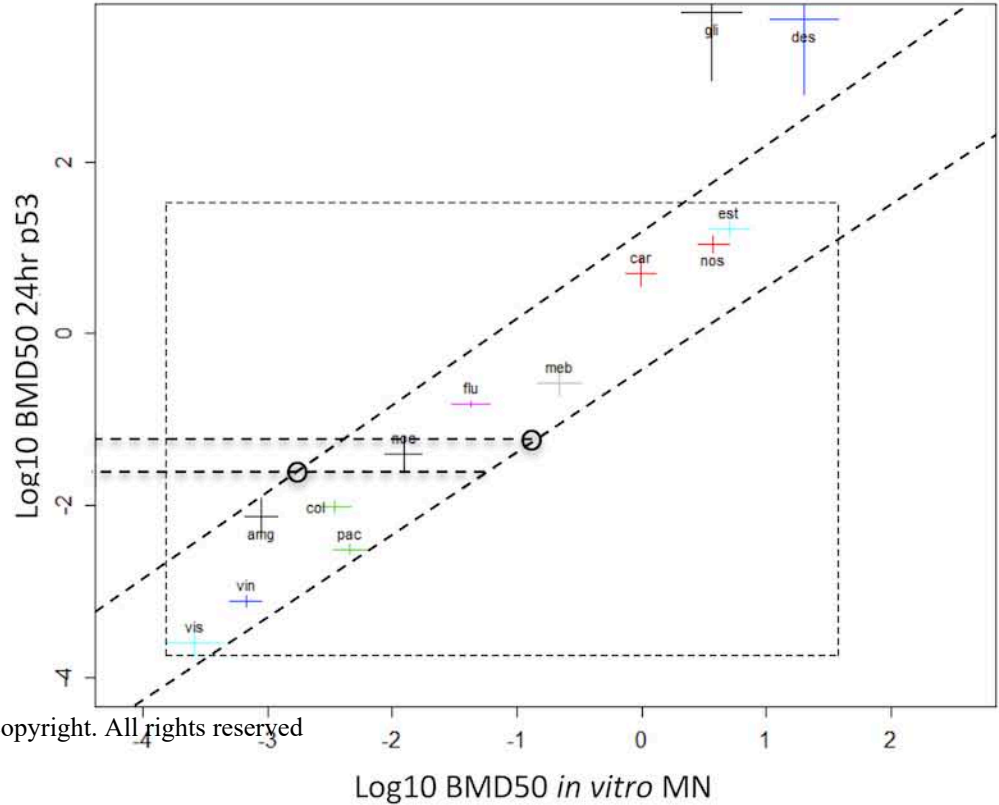
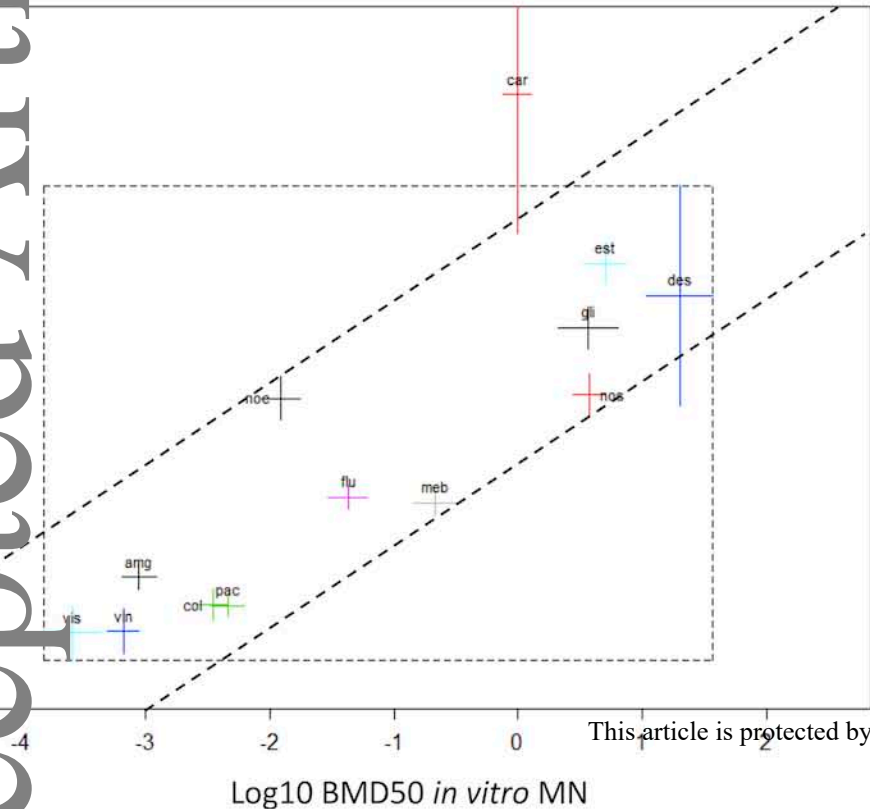


- 4-Nitroquinoline 1-oxide
- 1,3- Propane sultone
- N-Ethyl-N-nitrosourea
- MNNG
- Camptothecin
- Hydrogen peroxide
- 4d
- Etoposide
- Bleomycin sulfate
- Teniposide
- Mitoxantrone
- Topotecan
- Genistein
- Irinotecan
- Olaparib
- 5-Fluorouracil
- Apolizicidin
- Chlorambucil
- Methylmethanesulfonate
- Cisplatin
- Meprinan
- Mitomycin C
- Thiopypa
- 125
- Temozolamide
- Azathioprine
- AZD2858
- 221
- Menadiione
- Emodin
- Beta-Lapachone
- 1a
- 6-Thioguanine
- Azacitidine
- Glycylamide
- Dasatinib
- 9i
- Stavudine
- Hydralazine HCl
- Propylgallate
- Cytosine arabinoside
- Ethylmethanesulfonate
- Hydroxyurea
- Methotrexate
- Resorcinol diglycidyl ether
- Doxorubicin

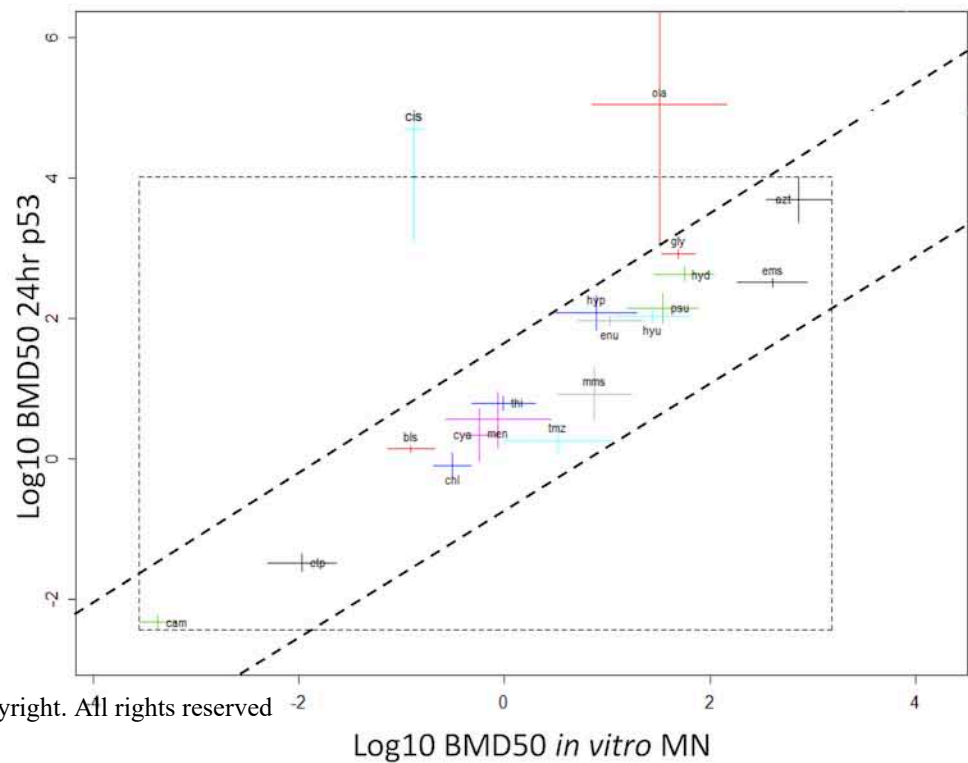
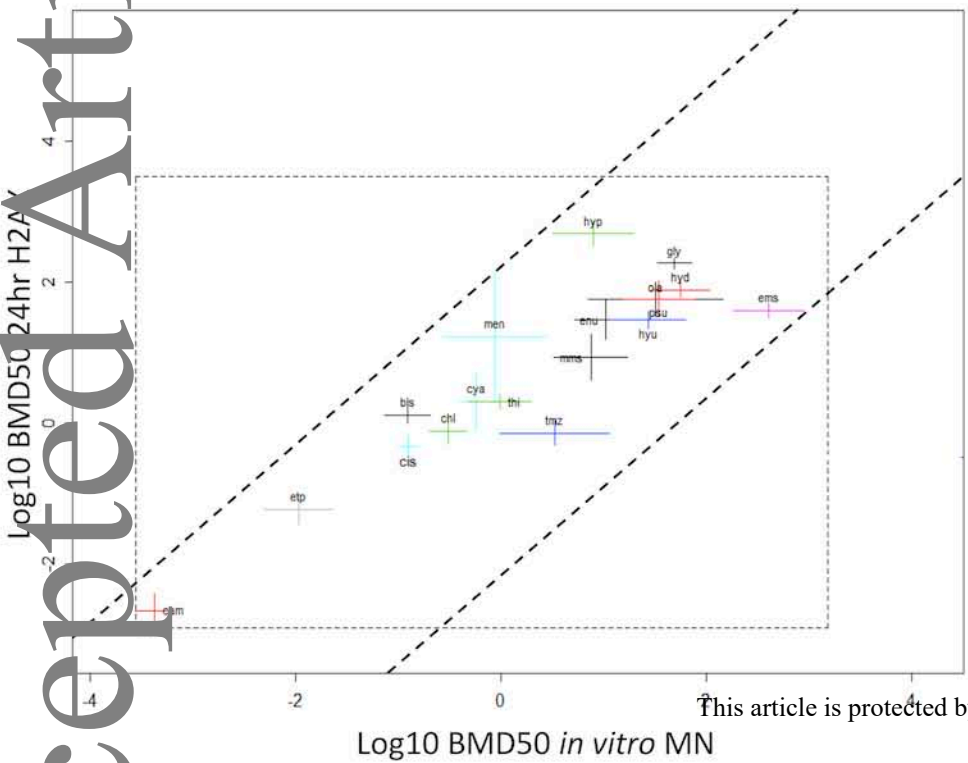


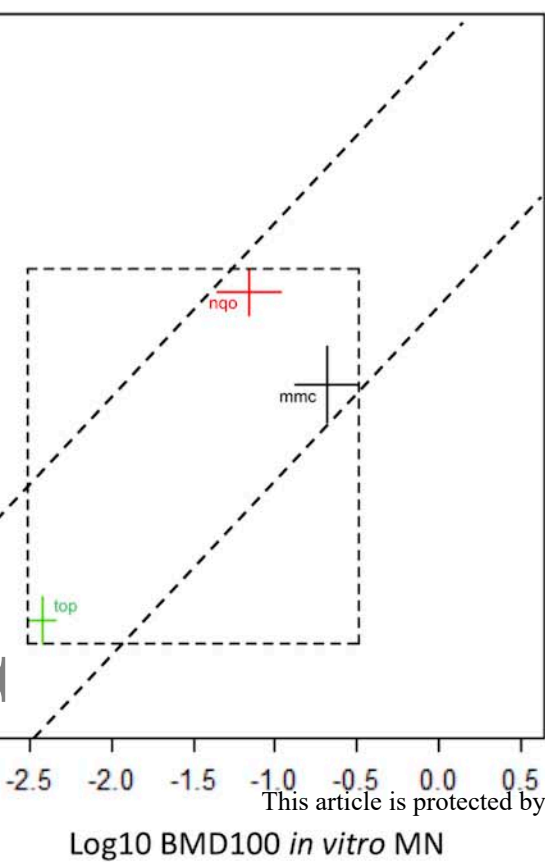
4 hr gH2AX (AUC)  
 4 hr p53 (AUC)  
 24 hr gH2AX (AUC)  
 24 hr p53 (AUC)











This article is protected by copyright. All rights reserved

